https://doi.org/10.5194/hess-2019-310
Preprint. Discussion started: 18 July 2019

Hydrology and Earth System Sciences
Discussions

Temperature controls production but hydrology controls export of dissolved organic carbon at the catchment scale

Hang Wen[1], Julia Perdrial[2], Susana Bernal[3], Benjamin W. Abbott[4], Rémi Dupas[5], Sarah E. Godsey[6], Adrian Harpold[7], Donna Rizzo[8], Kristen Underwood[8], Thomas Adler[2], Rebecca Hale[9], Gary Sterle[7], Li Li[1]*

[1]Department of Civil and Environmental Engineering, The Pennsylvania State University, University Park, PA 16802, USA
[2]Department of Geology, University of Vermont, Burlington, VT 05405, USA
[3]Center of Advanced Studies of Blanes (CEAB-CSIC), Accés Cala St. Francesc 14, 17300, Blanes, Girona, Spain
[4]Department of Plant and Wildlife Science, Brigham Young University, Provo, UT 84602, USA
[5]INRA, UMR1069 SAS, Rennes, France
[6]Department of Geosciences, Idaho State University, Pocatello, ID 83201, USA
[7]Department of Natural Resources and Environmental Science, University of Nevada, Reno, NV 89557, USA
[8]Department of Civil and Environmental Engineering, University of Vermont, Burlington, VT 05405, USA
[9]Department of Biological Sciences, Idaho State University, Pocatello, ID 83201, USA

Correspondence to: Li Li (lili@engr.psu.edu)

Abstract: Lateral carbon flux through river networks is an important and poorly-understood component of the global carbon budget. This work investigates how temperature and hydrology control the production and export of dissolved organic carbon (DOC) in the Susquehanna Shale Hills Critical Zone Observatory in Pennsylvania, USA. We applied the catchment-scale hydro-biogeochemical reactive transport model BioRT-Flux-PIHM to simulate the DOC dynamics. We estimated the daily DOC production rate (R_p; the sum of local DOC production rates in individual modeling grid cell) and the daily DOC export rate (R_e; the product of concentration and discharge at the stream outlet) to downstream ecosystems. Simulations showed that R_p varied by less than an order of magnitude and primarily hinged on seasonal temperature change. In contrast, R_e varied by more than three orders of magnitude with a strong dependence on discharge and hydrological connectivity. During summer, high temperatures led to high atmospheric water demand (and evapotranspiration) that dried and disconnected hillslope to stream. R_p

https://doi.org/10.5194/hess-2019-310
Preprint. Discussion started: 18 July 2019


Hydrology and Earth System Sciences
Discussions

reached its maximum but R_e was at its minimum. The stream only exported DOC from the organic-poor groundwater and from soil water in the narrow organic-rich swales with enriched DOC such that DOC accumulated in the catchment. During the wet period (winter and spring), R_p reached its minimum but R_e peaked because the stream was re-connected to a greater uphill area, flushing out the stored DOC. The model reproduced the observed concentration discharge (C-Q) relationship characterized by a flushing-dilution pattern with a rise in concentrations to a maximum (flushing) at a threshold discharge and then followed a general dilution with concentrations decreasing with discharge. This pattern was explained by the comparable contribution of organic-poor deeper groundwater and soil water from organic-rich swales at the minimum flow, maximized percentage contribution of soil water from organic-rich swales at the low flow regime, and increased contribution of uphill soil water interflow from uphill with less DOC at the high flow regime. This pattern persisted regardless of DOC production rate as long as the contribution of deeper groundwater flow remained low (<18% of the streamflow). When the groundwater flow increased to >18%, the flushing-dilution C-Q pattern shifted towards a flushing-only pattern with DOC concentrations increasing with discharge. This study illustrates the temporal asynchrony of DOC production, mostly controlled by temperature, and DOC export, primarily governed by hydrological flow paths at the catchment scale. The occurrence of warmer and more extreme hydrological events in the future could accentuate this asynchrony, with major lateral export of DOC dominated by a few major storm events whereas DOC is produced and stored in the catchment in the prolonged drought periods.

1. Introduction

Soil organic carbon (SOC) is the largest terrestrial stock of organic carbon, containing approximately four times more carbon than the atmosphere (Stockmann et al., 2013; Hugelius et al., 2014). Understanding the SOC balance requires consideration of lateral fluxes of carbon in water, e.g. dissolved organic and inorganic carbon (DOC and DIC), and vertical fluxes of carbon gases, e.g. CO_2 and CH_4 (Chapin et al., 2006). Both lateral and vertical carbon fluxes connect SOC with the atmosphere (Campeau et al., 2019), although lateral fluxes are arguably less understood and integrated into Earth system models (Aufdenkampe et al., 2011; Raymond et al., 2016). Lateral carbon fluxes from terrestrial to aquatic ecosystems are similar in magnitude to net vertical fluxes (Zarnetske et al., 2018; Regnier et al., 2013; Battin et al., 2009), highlighting the importance of understanding the controls of lateral carbon flux at multiple scales. In addition to its role in the global carbon cycle, DOC is an important water quality parameter that transports metals and contaminants, and imposes challenges for water

https://doi.org/10.5194/hess-2019-310
Preprint. Discussion started: 18 July 2019


Hydrology and Earth System Sciences
Discussions

treatment when concentrations are high (Sadiq and Rodriguez, 2004; Bolan et al., 2011). DOC also regulates food web structures by acting as an energy source for heterotrophic organisms and interacts with other biogeochemical cycles (Malone et al., 2018; Abbott et al., 2016a).

SOC decomposition and DOC production have been studied extensively (Abbott et al., 2015; Bernal et al., 2002; Hale et al., 2015; Neff and Asner, 2001; Humbert et al., 2015; Lambert et al., 2013). Despite their importance, the interactions between SOC and DOC and the response to climate change at catchment or larger scales remain unresolved (Kicklighter et al., 2013; Abbott et al., 2016b; Laudon et al., 2012; Clark et al., 2010; Evans et al., 2005). For example, some regions have experienced long-term increases in DOC concentrations, potentially due to recovery from acid rain or climate-induced changes in temperature (T) and catchment hydrological flow (Laudon et al., 2012; Perdrial et al., 2014; Evans et al., 2012; Monteith et al., 2007). Others have observed decreases or no changes (Skjelkvale et al., 2005; Worrall et al., 2018). More generally, the linkages among SOC processing, hydrological condition, and DOC export rates or concentration remain unclear. Two recent analyses indicate that the relationship between discharge (Q) and DOC concentration [DOC] (C) at stream outlets is primarily positive (Moatar et al., 2017; Zarnetske et al., 2018). Note that although the analyses in Zarnetske et al. (2018) was based on the relationship between Q and DOC flux, the transformation from DOC flux to C should still show the same general pattern for C-Q. Approximately 80% of watersheds in the U.S. and France show a C-Q flushing relationship (i.e. stream [DOC] increasing with discharge) while the rest show a general dilution (stream [DOC] decreasing with discharge) or chemostatic behavior (small concentration variation compared to discharge). These C-Q patterns are associated with different catchment characteristics, including slope and wetland area, and climate characteristics such as T (Moatar et al., 2017; Zarnetske et al., 2018). Meanwhile, the proximate hydrological and biogeochemical processes regulating SOC decomposition, DOC production, and DOC export remain uncertain (Jennings et al., 2010; Worrall et al., 2018), limiting response forecasts to future changes.

Stream DOC can be influenced by a variety of factors that control SOC decomposition and DOC production rates in soils at the local scale. These include climate factors such as T (Davidson and Janssens, 2006; Laudon et al., 2012), water content as a result of physical and chemical soil characteristics (Yan et al., 2018), and microbial and fungal activity (biological influence) (Brooks et al., 1999). These factors influence the SOC decomposition rate and DOC sorption on soils. DOC production generally increases as T increases; but there may be multiple thermal optima and further, the local rate of DOC production can vary with SOC characteristics, soil type, and the activity of soil biota (Davidson and Janssens, 2006; Jarvis and Linder, 2000; Yan et al., 2018). As the product of the stream discharge and [DOC], the DOC export rate at the catchment scale may be different from the DOC production rates at the local scale, which have been documented to be highly related to biogeochemical

https://doi.org/10.5194/hess-2019-310
Preprint. Discussion started: 18 July 2019


Hydrology and Earth System Sciences
Discussions

processes. For example, warm *T* can produce peak soil water [DOC] but cannot fully predict stream [DOC] and export rate, as the production and hydrological transport of DOC may not coincide in space and time (D'Amore et al., 2015). Because these drivers vary at the same time, it is difficult to identify which one dominates, creating substantial uncertainty in estimates of *T* and hydrological controls on DOC production and export.

In this context, we have developed a catchment-scale reactive transport model BioRT-Flux-PIHM (Biogeochemical Reactive Transport – Flux – Penn State Integrated Hydrologic Modeling System, BFP), hereafter referred to as BFP (Bao et al., 2017; Zhi et al., 2019). The model integrates catchment hydrological and biogeochemical processes. We used this model to explore the hydrological and *T* influence on DOC production and export at the catchment scale. We asked: *1. How do hydrology and T interact to determine DOC production and export at the catchment scale, 2. What determine the C-Q patterns observed at the outlet?* To answer these questions, we applied BFP to a temperate forest catchment in the Susquehanna Shale Hills Critical Zone Observatory (SSHCZO). We expected that *T* and soil moisture will drive DOC production in the soil, while DOC export from the catchment and thus the emergence of C-Q patterns, will be mostly related to hydrological connectivity. Therefore, the patterns of DOC production and DOC export might therefore be asynchronous (i.e. not happening at the same time) since they will respond differently to changes in *T* and hydrology.

2. Methods

2.1. Study site: the Shale Hills catchment with an intermittent stream

The Shale Hills catchment (0.08 km^2) is a V-shaped, first-order watershed with an intermittent stream in central Pennsylvania that situates on the Rose Hill Shale Formation. The average annual air *T* and precipitation are ~ 10 $^{\circ}C$ and 1000 mm in the past decade, respectively. The vegetation is deciduous forest, and the elevation ranges from 256 m a.s.l. at the catchment stream outlet to 310 m a.s.l. on the ridge (Figure 1A; Brantley et al., 2016). The watershed is characterized by large areas of swales and valley floors with deep and wet soils (Figure 1B). These soils contain more organic carbon (SOC, ~ 5% v/v) than hillslopes and uplands (~ 1% v/v) (Figure 1C).

https://doi.org/10.5194/hess-2019-310
Preprint. Discussion started: 18 July 2019

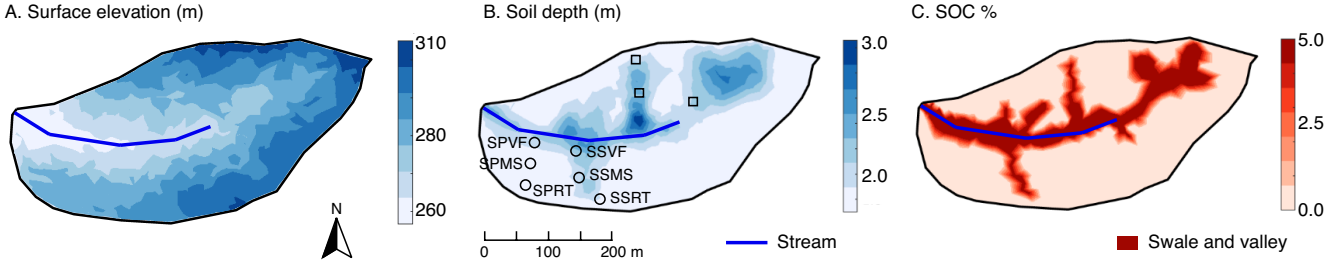

Figure 1. Map view of the SSHCZO with distributions of (A) surface elevation, (B) soil depth, and (C) soil organic carbon (SOC). Surface elevation was generated from LiDAR topographic data (criticalzone.org/shale-hills/data) while soil depths and SOC were interpolated using ordinary kriging based on field surveys with 77 and 56 sampling locations, respectively (Andrews et al., 2011; Lin, 2006). Note that the SOC distribution in Panel C is further simplified using the high, uniform SOC (5% v/v) in swales and valley soils based on field survey (Andrews et al., 2011). Swale and valley were defined based on surface elevation through field survey and 10-m resolution digital elevation model (Lin, 2006). Additional sampling instrumentation is shown in Panel B, including 6 soil water [DOC] (cycle) and 3 soil *T* (square) sampling locations. Soil water [DOC] was measured in lysimeter nests at the south planar sites – valley floor (SPVF), midslope (SPMS), and ridgetop (SPRT) and the swale sites - valley floor (SSVF), midslope (SSMS), and ridgetop (SSRT). Stream [DOC] was measured at the weir of the stream outlet. Real-time soil *T* (every 10 mins) was measured in the ridge top, midslope and valley floor, using automatic monitoring stations at depths of ~ 0.10, 0.20, 0.40, 0.70, 0.90, 1.00 and 1.30 m (Lin and Zhou, 2008).

2.2 The BFP model

BFP is a part of the general PIHM (Penn State Integrated Hydrologic Modeling System) family of code (Duffy et al., 2014). The code includes three modules (Figure 2): the surface hydrological module PIHM, the land-surface module Flux, and the multicomponent reactive transport module BioRT (Biogeochemical Reactive Transport). The code has been applied to simulate conservative solute transport, mineral dissolution, chemical weathering, surface complexation, and biogeochemical reactions at the catchment scale (Bao et al., 2017; Zhi et al., 2019; Li, 2019). Here we only introduce the salient features of the code that are relevant to this study; readers are referred to earlier publications for details on the code. Flux-PIHM distinguishes the subsurface flow into active interflow in shallow soil zones and groundwater flow deeper than the soil-weathered rock interface. The PIHM module simulates hydrological processes including precipitation, infiltration, surface runoff Q_S, soil water interflow (lateral flow) Q_L, and discharge Q (Figure 2). The Flux module simulates processes including solar radiation and evapotranspiration. Flux-PIHM calculates water variables (e.g. water storage, soil moisture, and water table depth) in unsaturated and saturated zones and assumes a no-flow boundary at the soil-bedrock interface with high

https://doi.org/10.5194/hess-2019-310
Preprint. Discussion started: 18 July 2019

permeability contrast. The deeper groundwater flow Q_G is estimated using the conductivity mass balance hydrograph separation (Lim et al., 2005).

The BioRT module takes in water calculated at each time step to simulate reactive transport processes, including advection, diffusion/dispersion, and biogeochemical reactions. The mass conservation governing equation for the reactive transport of a single solute m is as follows:

$$V_i \frac{d(S_{w,i}\theta_i C_{m,i})}{dt} = \sum_{j=N_{i,1}}^{N_{i,x}} \left(A_{ij} D_{ij} \frac{C_{m,j} - C_{m,i}}{l_{ij}} - q_{ij} C_{m,j} \right) + r_{m,i}\,, \quad m = 1, np \qquad (1)$$

Here, the subscripts i, j represent the grid block i and the neighboring grid j, respectively; the subscript x distinguishes between flow in the unsaturated zone (infiltration and recharge) and saturated zone (recharge and lateral flow); V is total bulk volume (m^3) of each grid block; S_w is soil moisture (m^3 water/m^3 pore volume); θ is porosity; C is aqueous species concentration (mol/m^3 water); t is time (s); N is the index of elements sharing surfaces; A is the grid interface area (m^2); D is diffusion/dispersion coefficient (m^2/s); l is the distance (m) between the center of two neighboring grid blocks; q is the flow rate (m^3/s); r_m is the kinetically controlled reaction rates (mol/s) involving species m, which is the DOC production rate from SOC decomposition at the grid block i in this work; np is the total number of independent solutes.

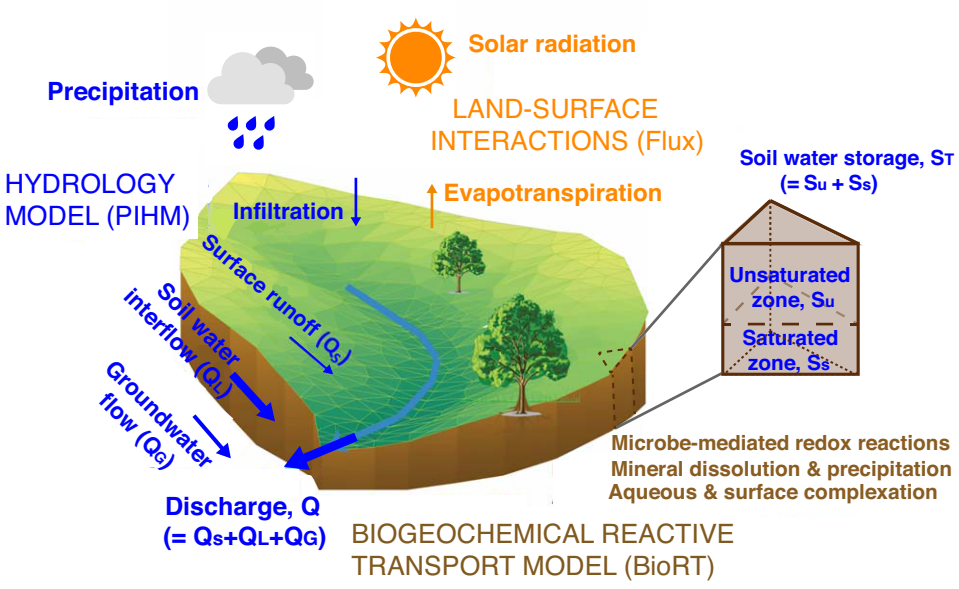

Figure 2. A schematic representation of major processes in the catchment-scale reactive transport model BFP. Stream discharge Q sources from surface runoff Q_S, soil water interflow (lateral flow) Q_L, and

https://doi.org/10.5194/hess-2019-310
Preprint. Discussion started: 18 July 2019

Hydrology and Earth System Sciences
Discussions

groundwater flow Q_G. Soil water storage S_T is the sum of soil water in the unsaturated (S_u) and saturated zone (S_s). At Shale Hill, on the annual basis, the soil water interflow contributes about 90% to stream discharge, whereas groundwater flow and surface runoff contributes about 8% and 2%, respectively.

DOC production and sorption. In the model, DOC is produced by the decomposition of SOC via the kinetically-controlled reaction $SOC(s) \rightarrow DOC$. With abundant SOC and O_2 in soils serving as electron donors and acceptors, a simplified form of the dual Monod kinetics is used:

$$r_p = kAf(T)f(S_w) \qquad (2)$$

Here r_p is local DOC production rate and equivalent to r_m in Eq. (1), where m is DOC. k is the kinetic rate constant of net DOC production (= 10^{-10} mol/m^2/s); A is the SOC surface area (m^2, = 2.5×10^{-3} m^2/g × g of SOC mass) which essentially lumps SOC content and biomass abundance. The functions $f(T)$ and $f(S_w)$ describe the rate dependence of r_p on soil T and moisture, respectively. $f(T)$ follows a widely-used Q_{10}-based formation: $f(T) = Q_{10}^{|T-10|/10}$, where Q_{10} is the factor by which the reaction rate increases with T, and the number 10 in the superscript represents the reference T of 10 °C (Davidson and Janssens, 2006). Q_{10} in the base case is set at 2.0, within the typical range of 1.2-3.8 for forest ecosystems (Liu et al., 2017). The $f(S_w)$ has the form $f(S_w) = (S_w)^n$ in the base case, where n is the saturation exponent with a value of 1.0 (Yan et al., 2018). The dependence of local production rates on soil T and moisture have been described with multiple forms in existing studies (Davidson and Janssens, 2006; Yan et al., 2018) and will be further explored through sensitivity analysis, detailed in Section 2.6. The SOC content typically decreases with depth (Billings, 2018; Bishop et al., 2004). To take this into account, we use the equation $C_d(z) = C_0 exp\left(-\frac{z}{b_m}\right)$, where C_d is SOC at depth z below the surface; C_0 is the SOC level at the ground surface and b_m reflects the decline with depth, set here to a value of 0.3 (Weiler and McDonnell, 2006).

DOC produced from SOC can also sorb on soils via the reaction $\equiv X + DOC \leftrightarrow \equiv XDOC$, where $\equiv X$ and $\equiv XDOC$ represents the functional group that can sorb DOC and the functional group with sorbed DOC, respectively (Rasmussen et al., 2018). This reaction is considered fast and is thermodynamically-controlled such that an equilibrium constant K_{eq} links the activity (here approximated by concentrations) of the three chemicals via $K_{eq} = \frac{[\equiv XDOC]}{[\equiv X][DOC]}$. The concentrations of DOC calculated from solving Eq. (1) are used to calculate the concentrations of $\equiv X$ and $\equiv XDOC$. The K_{eq} value represents the thermodynamic limit of the sorption reaction, i.e., the sorption capacity of the soil for DOC. The value of K_{eq} is $10^{0.2}$ in this work, obtained by fitting the stream and soil [DOC] data (detailed in Section 2.4).

https://doi.org/10.5194/hess-2019-310
Preprint. Discussion started: 18 July 2019


Hydrology and Earth System Sciences
Discussions

2.3 Domain setup

BFP is a 2.5D model with full discretization in the horizontal directions and discrete discretization in the vertical direction with three layers: ground surface, unsaturated, and saturated zones. The study watershed is discretized into 535 prismatic land elements and 20 stream segments using PIHMgis (http://www.pihm.psu.edu/pihmgis_home.html), a GIS interface that is tightly coupled to BFP. The land elements are unstructured triangles with mesh sizes varying from 10 to 100 m. The simulation domain is set up using national datasets, including the USGS National Elevation Dataset for topography, the National Land Cover Database for land cover, the National Hydrography Dataset, the North American Land Data Assimilation Systems phase 2 (NLDAS-2) for hourly meteorological forcing, and the Moderate Resolution Imaging Spectroradiometer (MODIS) for leaf area index every eight days. In addition, extensive characterization and measurement data at Shale Hills have been used to define soil properties, water chemistry, and mineralogy that are heterogeneously distributed across the catchment (Andrews et al., 2011; Lin, 2006; Jin and Brantley, 2011; Jin et al., 2010; Shi et al., 2013). This includes the soil depth in Figure 1, soil properties (e.g. soil type, soil hydraulic conductivity, macro pore conductivity, porosity, and van Genuchten parameters), initial water conditions, among other field measurements at Shale Hills (criticalzone.org/shale-hills/data/).

Based on field measurements that swales and valley has relatively high SOC (Andrews et al., 2011), the spatial distribution of SOC (Figure 1C) is simplified with high, uniform SOC in swales and valley (5% v/v solid phase) compared to 1% in the rest of the catchment. The spatial distribution of clay minerals is characterized from field measurements, with a value of 23% v/v solid phase along the ridgetop and increasing to 33% at valley floor (Jin et al., 2010; Li et al., 2017). The input DOC concentrations in rainfall and groundwater (below soils) are set as constants using reported median values of 0.6 and 1.2 mg/L, respectively (Andrews et al., 2011; Iavorivska et al., 2016), as high frequent DOC observations for rainfall and groundwater are not available at the site. The initial DOC soil water concentration is set as 2.0 mg/L, the average concentration from six field sampling locations.

2.4 Model calibration

We used stream (daily) and soil pore water (biweekly) [DOC] data during April-October 2009 for model calibration. We used the year 2008 as spin-up and ran the model until steady state for both water and chemical solute. The model performance was evaluated using the monthly Nash-Sutcliffe efficiency (NSE) (Nash and

https://doi.org/10.5194/hess-2019-310
Preprint. Discussion started: 18 July 2019


Hydrology and Earth System Sciences
Discussions

Sutcliffe, 1970). NSE quantifies the relative magnitude of residual variance of modeling output compared to measurements. The general satisfactory range for monthly-average outputs for hydrological models is NSE > 0.5 (Moriasi et al., 2007) and we used similar standards for biogeochemical solutes (Li et al., 2017). The calibration of Flux-PIHM was based on previous work using multiple field measurements in 2009 (Shi et al., 2013), including daily discharge, soil moisture, water table depth, and surface heat fluxes. In this work, groundwater estimates were further refined by first calculating average groundwater fluxes in wet and dry periods using the conductivity mass balance hydrograph separation (Lim et al., 2005) and then iteratively calibrating between discharge and stream chemistry to reproduce discharge and stream [DOC] simultaneously. In other words, stream chemistry helps to constrain the groundwater flow into the stream.

In reproducing the [DOC] data, we also tuned the SOC surface area A for DOC production rates (Eq. (2)) and the equilibrium constant K_{eq} for DOC sorption. Because not all soils are in contact with water, the calibrated surface area represents the effective reactive solid-water contact area in heterogeneous subsurface, and is orders of magnitude lower than the reported SOC surface areas at laboratory experiments (Lawrence et al., 2015), consistent with other observations scaling off the surface area for mineral dissolution/weathering (e.g., Li et al. (2014)).

2.5 Quantification of water and DOC dynamics at the catchment scale

Hydrological connectivity. Modeled spatial and temporal outputs of saturated soil water storage were used to quantify hydrological connectivity ($I_{cs}/Width$), an emergent quantity at the catchment scale. I_{cs} (m) is the average width of the catchment connected to the stream in the direction perpendicular to the stream channel while the *Width* is the average width of catchment in the direction perpendicular to the stream (230 m). The term $I_{cs}/Width$ quantifies the average proportional width of the catchment connected to the stream (e.g., $I_{cs}/Witdh$ = 0.10, 0.35, and 0.70 in Figure S1). Depending on the catchment geometry and extent of connectivity, $I_{cs}/Width$ may vary from 0 to 1.0. Note that $I_{cs}/Width$ may exceed 1.0 for catchments with the length >> width under extreme precipitation events. High $I_{cs}/Width$ value (i.e., high hydrological connectivity) indicates that a large catchment area is connected to the stream. To determine whether two land elements are hydrologically connected, the spatial distribution of saturated water storage was used following $I_{cs} = \int_0^\infty \tau(h)dh$ based on algorithm in (Allard, 1994; Western et al., 2001; Xiao et al., 2019). Here $\tau(h)$ is the probability of two grid blocks being connected at a separation distance of h, in which a threshold is defined as the 75th percentile of saturated storage over the whole catchment (Western et al., 2001;

https://doi.org/10.5194/hess-2019-310
Preprint. Discussion started: 18 July 2019


Hydrology and Earth System Sciences
Discussions

Xiao et al., 2019). Note that $I_{cs}/Width$ here only quantifies the hydrological connectivity in soils and does not reflect the groundwater in shallow aquifers below the soil-bedrock interface.

DOC at the catchment scale. At the catchment scale we differentiate two different rates (mg/d): DOC production and export. The production rate R_p is the sum of the local DOC production rate r_p in individual grid blocks (Eq. (2)) across the whole catchment. The DOC sorption is included in the production, although some of the produced DOC sorbs on soils. The export rate R_e is calculated as the product of discharge and [DOC] at the stream outlet. For the DOC mass balance calculation, total stored DOC is the difference between input from production, rainfall, and groundwater and output (stream export). The DOC input from the rainfall R_r (mg/d) is the precipitation rate (m/d) times the rainfall [DOC] (0.6 mg/L) and the catchment drainage area (m^2). The DOC input from groundwater R_g (mg/d) is the total groundwater influx (groundwater flow rate × catchment drainage area) times the groundwater [DOC] (1.2 mg/L).

C-Q patterns were quantified using the power law equation $C = aQ^b$ (Godsey et al., 2009) and the ratio of coefficient of variations of [DOC] and discharge $\frac{CV_{[DOC]}}{CV_Q}$ (Musolff et al., 2015). We categorized 3 possible categories based on these metrics (Godsey et al., 2009; Underwood et al., 2017; Musolff et al., 2015): If b falls between -0.2 and 0.2 and $\frac{CV_{[DOC]}}{CV_Q} < 1$, it is chemostatic (i.e. relatively small variation of concentration compared to discharge). Values of b>0.2 and $\frac{CV_{[DOC]}}{CV_Q} < 1$ indicate flushing, while values of b < -0.2 and $\frac{CV_{[DOC]}}{CV_Q} < 1$ indicate dilution. We used the Matlab curve-fitting toolbox to obtain both the best fit model parameters and the goodness-of-fit measures, including confidence intervals and the R^2 statistic.

2.6 Sensitivity analysis

We used a sensitivity analysis to explore the influence of soil T and moisture on [DOC] and DOC production and export rates (R_p and R_e). The Q_{10} in the temperature-dependence function $f(T) = Q_{10}^{|T-10|/10}$ was explored using the minimum value of 1.0 (i.e. no dependence on T) and the maximum value of 4.0 (Davidson and Janssens, 2006) (Figure S2A), i.e. $f(T) = 1$ and $f(T) = 4^{|T-10|/10}$. The rate dependence on soil moisture was explored using the base case $f_1(S_w) = (S_w)^n$ (increase behavior), and three additional functions (f_2, f_3, and f_4)

https://doi.org/10.5194/hess-2019-310
Preprint. Discussion started: 18 July 2019


Hydrology and Earth System Sciences
Discussions

representing the most commonly observed forms (Figure S2B), including decrease behavior, constant behavior, and threshold behavior (Gomez et al., 2012; Yan et al., 2018):

$$\text{Decrease-behavior function} \quad f_2(S_w) = \left(\frac{1-S_w}{0.6}\right)^{0.77} \tag{3}$$

$$\text{Constant-behavior function} \quad f_3(S_w) = 0.65 \tag{4}$$

$$\text{Threshold-behavior function} \quad f_4(S_w) = \begin{cases} \left(\frac{S_w}{0.7}\right)^{1.5} & S_w \le 0.7 \\ \left(\frac{1-S_w}{1-0.7}\right)^{1.5} & S_w > 0.7 \end{cases} \tag{5}$$

The constants in Eq. (3)-(5) were selected to ensure similar averages of $f(S_w)$ across the whole S_w range such that trajectories rather than absolute values of $f(S_w)$ were compared (Figure S2B).

We also tested the sensitivity of DOC sorption onto soils by changing K_{eq} between values of 0 (no sorption), 0.5 and 1.0. As an important source of stream water and DOC, the sensitivity of C-Q patterns and R_e to changes in groundwater was also tested. First, we varied the groundwater flow contribution to stream discharge from negligible to 18.8% of the total streamflow (Q_G/Q = 0 and 18.8%). Second, we varied the groundwater [DOC] by two orders of magnitude (0.12 mg/L and 12.0 mg/L). We compared results from these analyses to the base case for which the groundwater contributed to a 7.5% of the total annual streamflow.

3. Results

3.1. Processes and dynamics in the base case

Water dynamics. The total precipitation from 1 April 2009 to 31 March 2010 was 1,130 mm. Measured stream discharge Q at Shale Hills (Figure 3) was highly responsive to intense precipitation events and was high (~ 10^{-2} m/day) in spring and fall compared to summer with high soil T and high ET (~ 10^{-5} m/day). The model captured the temporal dynamics of daily discharge, ET, and soil T with an NSE value of 0.68, 0.72, and 0.62, respectively (Figure 3A-B). The model estimated that 47.5% of annual precipitation contributed to discharge while the rest to ET. The stream discharge Q has three components, including surface runoff Q_S, soil water interflow Q_L (lateral flow) and groundwater flow Q_G below the soil-weathered rock interface (Figure 2). On average, about 92.5% of discharge Q was from lateral flow Q_L (90.2%) and surface runoff Q_S (2.3%). Q_G was estimated as 1.3×10^{-4} and 4.0×10^{-5} m/day for the wet and dry periods (August – September), respectively, following the conductivity mass balance hydrograph separation (Lim et al., 2005). Q_G accounted for ~ 7.5% of the annual average stream discharge, similar to previously reported values (Li et al., 2017; Hoagland et al., 2017). In the dry months from August to

https://doi.org/10.5194/hess-2019-310
Preprint. Discussion started: 18 July 2019

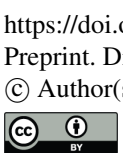

Hydrology and Earth System Sciences
Discussions
Open Access
EGU

September, the stream was almost dry with no visible flow. During this period, the relative contribution of groundwater to *discharge* was similar with that of that of the soil lateral flow (Figure 3B).

In fact, as the unsaturated water storage S_u was often more than 10 times larger than the saturated storage S_s, the total soil water storage S_T and S_u curves almost overlapped (Figure 3C). S_s was negligible in the dry period (close to 0 m), contributing little flow to the stream. Hydrological connectivity ($I_{cs}/Width$) covaried with S_T but showed significant temporal fluctuations. Generally, the dry period had small S_T, low connectivity and low discharge. In other words, high summer ET coincided with expanding and shrinking the connected zone of the catchment.

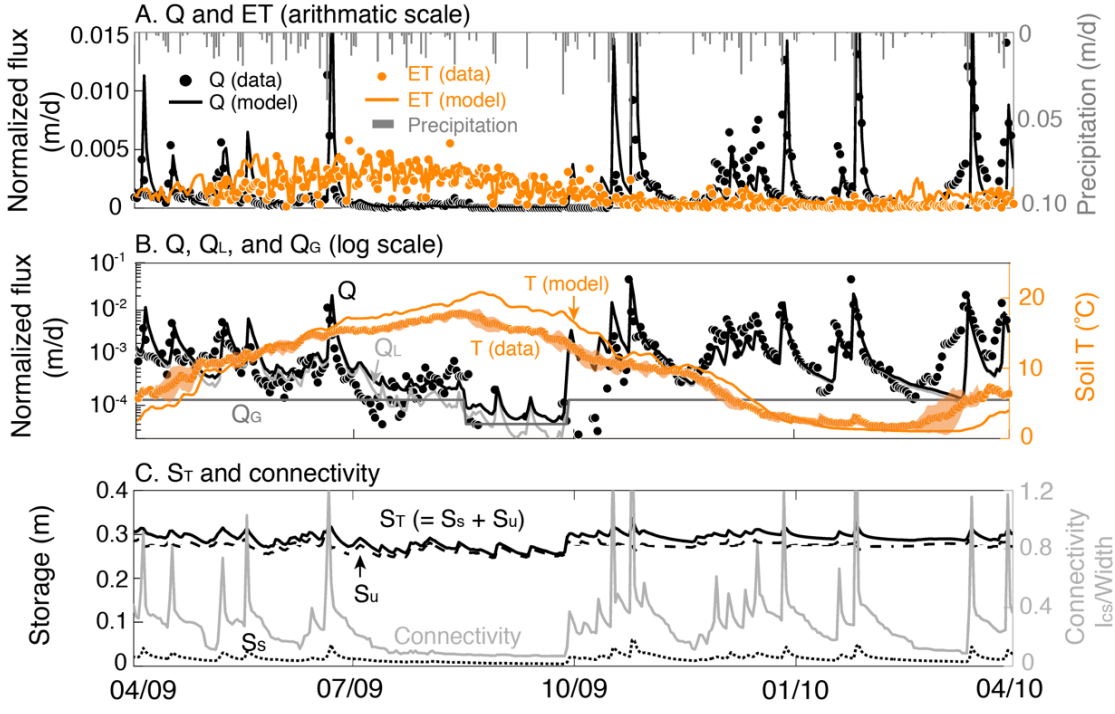

Figure 3. Temporal dynamics of (A) daily precipitation, stream discharge Q, and evapotranspiration ET on an arithmetic scale; (B) stream discharge Q, soil water interflow Q_L, and groundwater Q_G on a logarithmic scale and soil T on an arithmetic right axis; (C) soil water storage S_T and hydrological connectivity $I_{cs}/Width$. The yellow dots in Panel B represent the average soil T from 3 sampling locations (square symbols in Figure 1B) while the shaded zone is the measurement variation. Q was highly responsive to intense precipitation events in spring and winter. Note high soil T, high ET, low S_T and low $I_{cs}/Width$ during July-August 2009. Stream discharge was primarily comprised of Q_L, except in July-October when the relative contribution of Q_G increased.

https://doi.org/10.5194/hess-2019-310
Preprint. Discussion started: 18 July 2019

Hydrology and Earth System Sciences
Discussions
Open Access
EGU

Temporal patterns of DOC concentrations. The model captured the general trend of stream [DOC] (NSE = 0.55 for monthly [DOC]) (Figure 4). A temporal pattern emerged from changes in the relative contribution of soil water Q_L and groundwater Q_G to stream discharge Q over time. Under low discharge conditions, Q_G contributed substantially to Q (~32-71%) (Figure 3); and stream [DOC] reflected the mixing of groundwater and soil water (Figure 4A). Under high discharge conditions, stream [DOC] instead mirrored soil water [DOC] that was exported to the stream (light blue line), indicating the dominant contribution of Q_L to Q. The simulated soil water [DOC] at local scales matched well the corresponding field data at the six sampling locations with NSE = 0.52 (Figure 4B-G), which showed relatively less temporal variation than stream [DOC]. This is likely because it took time to transport DOC through the catchment; and these local scales were not always hydrologically connected to the stream.

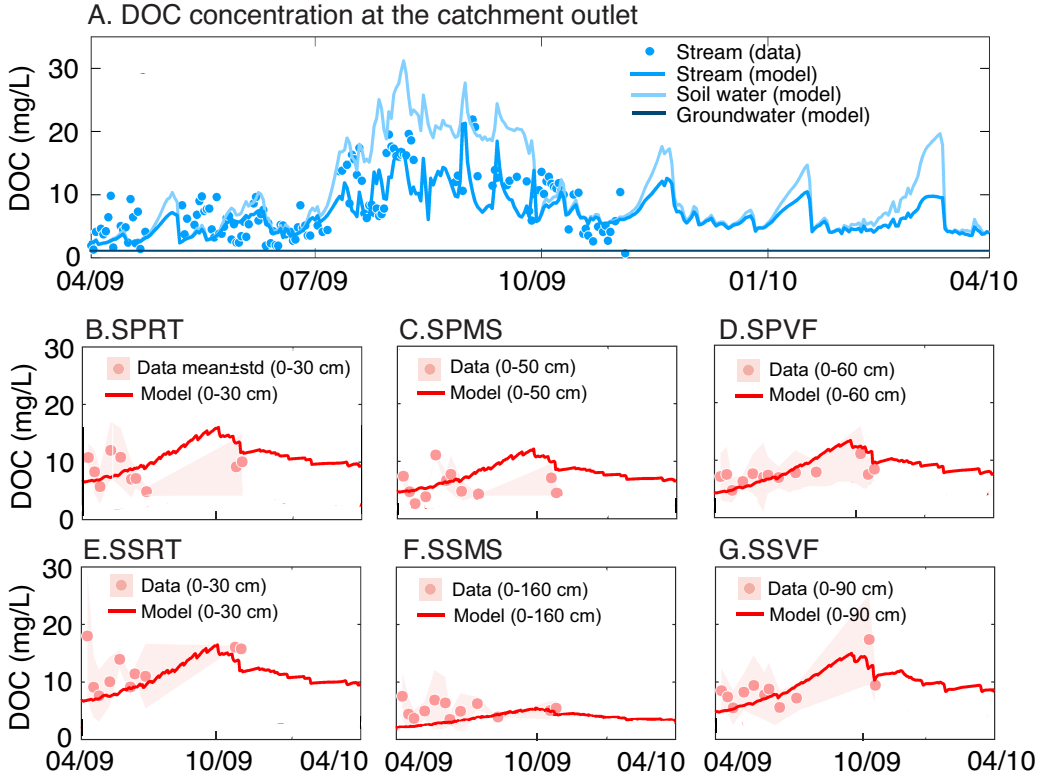

Figure 4. (A) Temporal dynamics of measured and simulated stream [DOC] as well as groundwater and soil water [DOC]. Simulated stream DOC (bright blue line) was contributed by exported DOC from the soil water Q_L (light blue line) and groundwater Q_G (dark blue line). Under low discharge conditions (e.g., July-September in Figure 3), Q_G contributed a larger proportion of discharge and stream DOC whereas under high discharge conditions, stream DOC was dominated by the contribution of DOC from Q_L. (B)-

https://doi.org/10.5194/hess-2019-310
Preprint. Discussion started: 18 July 2019

Hydrology and Earth System Sciences
Discussions

(G) Local soil water [DOC] for the 6 sampling locations shown in Figure 1B, including 3 planar (panels B-D) and 3 swale locations (panels E-G).

Spatial patterns and mass balance. Figure 5 shows the spatial patterns and its possible controls in May (wet), August (dry) and October (wet after dry). In May, the average soil T was around 12 °C with relatively minor variations (< 3 °C) across the catchment. Most convergent areas including the main stream valley and swales were well connected to the stream and had high water content (Figure 5B-C). The distribution of local production rates r_p (Figure 5D) and soil water [DOC] (Figure 5E) followed that of SOC (Figure 1C) and water content (Figure 5B), with high r_p and soil water [DOC] in swales and valley with relatively high water and SOC contents. Low r_p in relatively dry planar hillslopes and uplands led to low soil water [DOC]. In August, the average soil T increased to around 20°C. The hydrologically connected zones shrank to the immediate vicinity of the stream, but r_p increased (about 2× from May) at this higher temperature. Soil water [DOC] also increased by a factor of 2 with the highest r_p and still concentrated in swales and valley, including hillslope and uplands, partly because the produced DOC was trapped in these areas that were not connected to the stream. In October, r_p decreased as soil T cooled compared to summer. But increased precipitation and decreased ET changed spatial pattern of connectivity: the hydrologically connected zones expanded beyond swales and valley to include more of the upland hillslopes (Figure 5C). The increase in hydrological connectivity favored the flushing of some of the DOC stored in soils, although the soil water [DOC] still remained high due to the legacy of produced DOC from antecedent dry times.

https://doi.org/10.5194/hess-2019-310
Preprint. Discussion started: 18 July 2019

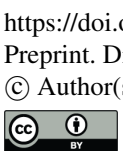

Hydrology and Earth System Sciences
Discussions
Open Access
EGU

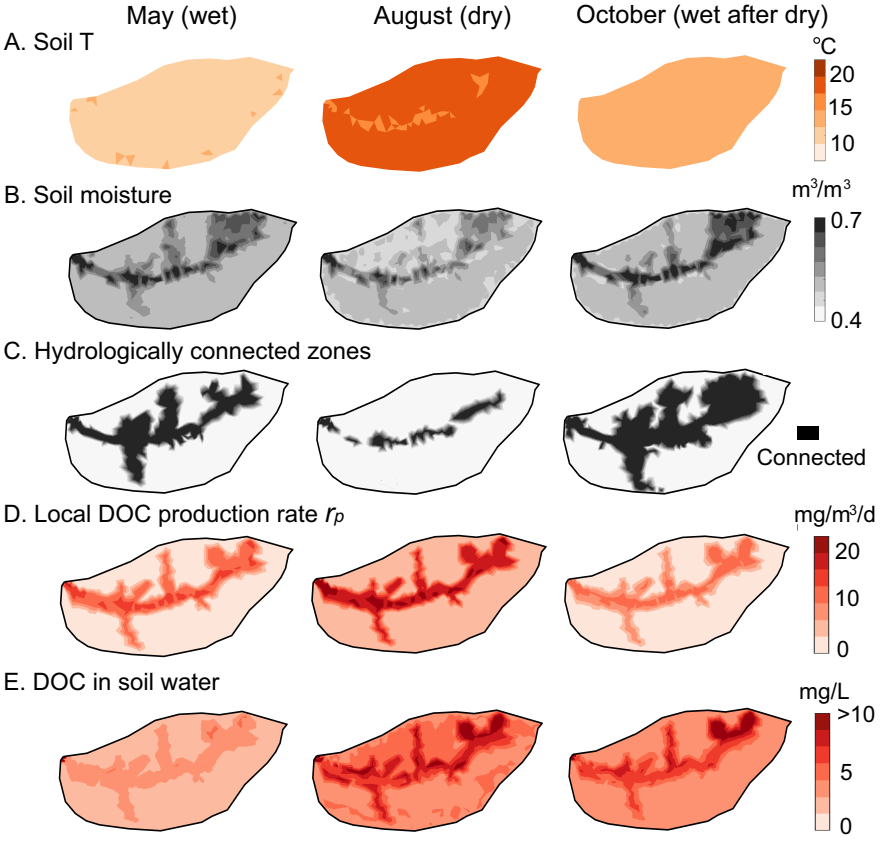

Figure 5. Spatial profiles in May (wet), August (dry), and October (wet after dry) of 2009: (A) soil *T*, (B) soil moisture, (C) hydrologically connected zones, (D) local DOC production rates r_p and (E) soil water [DOC]. The soil [DOC] and r_p are high in swales and the main valley that have relatively high soil water and SOC content (Figure 1C). Although water content in August is relatively low compared to May and October, higher soil *T* leads to higher r_p, with most DOC production and accumulation in zones that are disconnected to the stream.

Figure 6 shows the catchment-scale DOC production and export rates and DOC mass balance. Generally, the average daily R_p (5.1×10^5 mg/d) was greater than the daily contribution from either rainfall R_r (1.6×10^5 mg/d) or groundwater R_g (1.2×10^4 mg/d), respectively. During storm events, R_r occasionally exceeded R_p. R_p was generally high in summer, despite low water storage. Export rate R_e did not follow the temporal patterns of either the total input rate ($R_p+R_r+R_g$) or R_p. Instead, it primarily followed the discharge patterns: large rainfall events exported disproportionally high DOC, leading to abrupt drops in DOC mass remaining in the catchment. From the wet to dry period, as water levels dropped, DOC accumulated within the catchment (Figure 5E, May to August). During the dry-to-wet transition, as the catchment became wetter, the contributing areas expanded to uplands and

https://doi.org/10.5194/hess-2019-310
Preprint. Discussion started: 18 July 2019

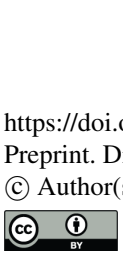

the DOC was flushed out of the catchment, decreasing the overall DOC soil pool to lower values (Figure 5E, August-October).

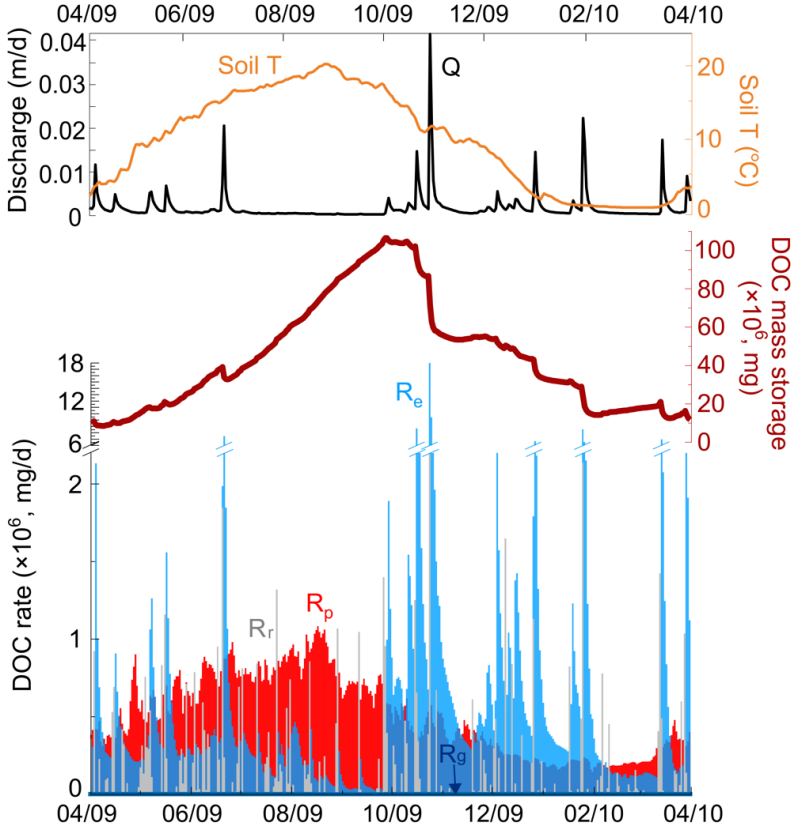

Figure 6. Temporal dynamics of DOC mass storage in Shale Hills and corresponding DOC influent rate (rainfall R_r, groundwater R_g, production R_p) and outflow (effluent R_e) rate. The stored DOC mass in the catchment was calculated as (DOC influent rate - outflow rate) × time). The DOC production from soil decomposition is the major DOC source at Shale Hills. The temporal R_e dynamics mostly followed the trend of discharge while R_p mostly followed the trend of soil T.

C-Q patterns and rate dependence. The C-Q relationships showed an unusual pattern (called as the chevron pattern in Meybeck and Moatar (2012)) with a positive correlation at low Q followed by a negative correlation at higher Q (Figure 7A). The simulated DOC C-Q relationship captured this unusual trend. The C-Q relationships showed a general dilution behavior with the C-Q slope b = -0.23 and $\frac{CV_{[DOC]}}{CV_Q}$ = 0.22, consistent with the general pattern exhibited in the field data (Figure 7A). This C-Q pattern can be explained by the dynamics of different

https://doi.org/10.5194/hess-2019-310
Preprint. Discussion started: 18 July 2019

Hydrology and Earth System Sciences
Discussions

water sources with different DOC content contributing to the stream. At low discharges (< 1.8×10^{-4} m/d) with small water storage (0.25-0.28 m) and connectivity ($I_{cs}/Width$ <0.1) (Figure 7B), the stream DOC was mainly from the organic-rich swales and valley floor zones. At higher discharges with connectivity exceeding 0.1, soil water [DOC] decreased due to the contribution of water from planar hillslopes and uplands, leading to the decrease of stream [DOC] and a dilution C-Q pattern. Daily R_e correlated positively with S_T, hydrological connectivity and Q, and increased over two orders of magnitude with a three-order-of-magnitude increase in Q. The variation of daily R_p with Q was small (10^5 -10^6 mg/d) compared to that of R_e (Figure 7B).

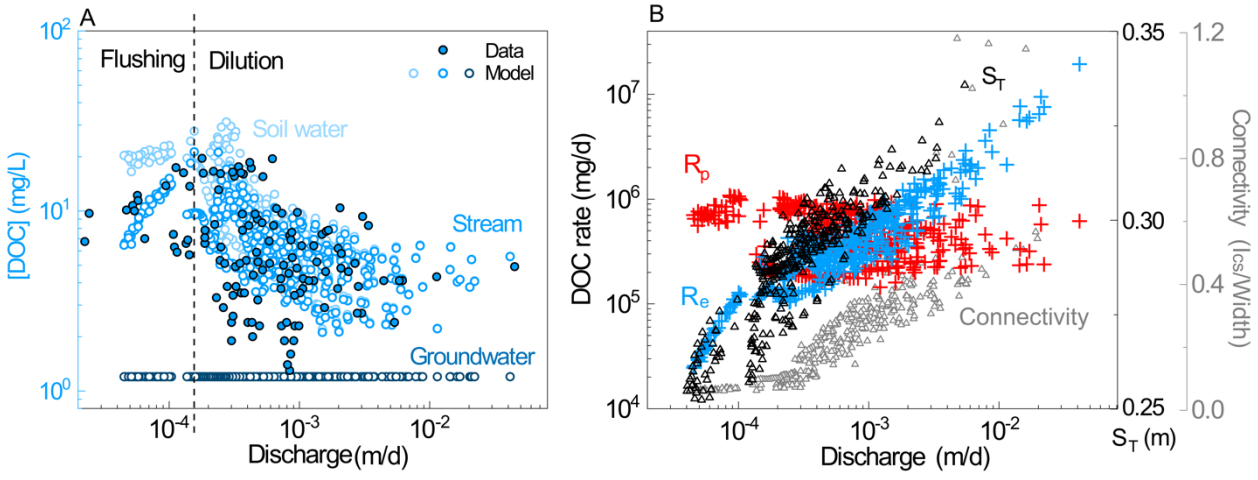

Figure 7. Relationships of daily discharge Q with: (A) stream [DOC]; open circles are simulations; filled circles with a black outline are data; (B) soil water storage S_T, connectivity ($I_{cs}/Width$) and DOC rates (R_e and R_p). At low discharges (< 1.8×10^{-4} m/d), the stream DOC was sourced mainly from the valley floor, characterized by high SOC decomposition rates and soil water [DOC], leading to a flushing (positive) pattern. At higher discharges, the relative contribution of water from planar hillslopes and uphills with low soil water [DOC] increased, plummeting the stream [DOC] to lower concentrations resulting in a dilution (negative) C-Q pattern. R_e increased by two orders of magnitude with increasing Q, while R_p varied within an order of magnitude.

R_p depended more on soil T compared to soil water storage S_T and hydrological connectivity ($I_{cs}/Width$). In contrast, R_e increased with soil water storage S_T but notably decreased with soil T (> 17 ºC), likely because of the low discharge during the hot and dry summer.

https://doi.org/10.5194/hess-2019-310
Preprint. Discussion started: 18 July 2019

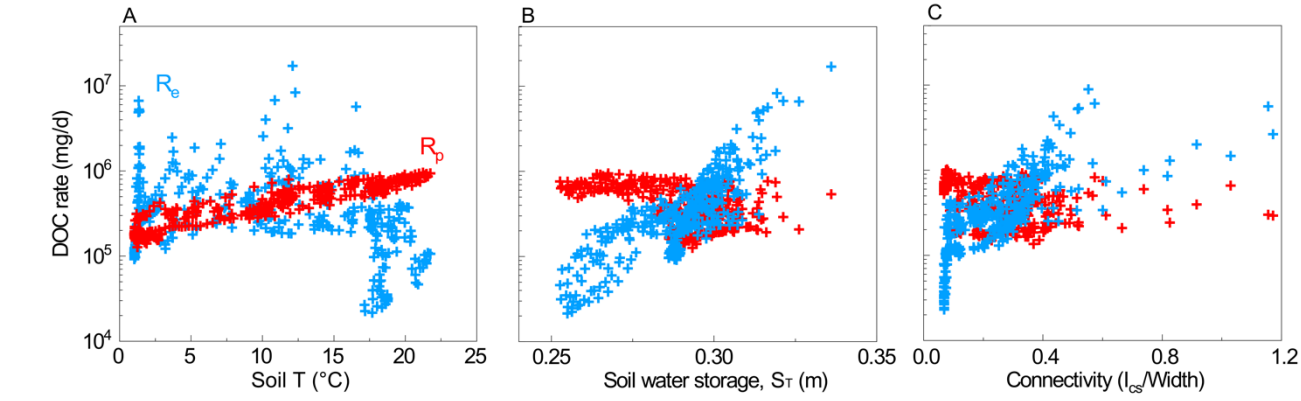

Figure 8. Catchment-scale DOC production rate R_P and export rate R_e as a function of (A) soil T, (B) soil water storage S_T, and (C) hydrological connectivity (l_{cs}/*Width*). Dots represent daily outputs of the base case where the local DOC production rate r_p (Eq. (2)) was assumed to be dependent on soil temperature $f(T) = 2^{|T-10|/10}$ and soil moisture $f(S_w) = (S_w)^{1.0}$, respectively. R_p increased with soil T and decreased slightly with S_T and connectivity. In contrast, R_e increased with S_T and connectivity but decreased with soil T. R_e tended to decrease with soil T in the hot, dry summer because of extremely low discharge that occurred at that period.

3.2. Sensitivity analysis

Control of temperature, soil moisture, and sorption on DOC production and export. Higher Q_{10} values in *f(T)* leads to more pronounced seasonality in R_p (Figure 9A). The R_p for Q_{10}=4.0 was more than 4 times higher than that of Q_{10}=1.0 in summer, while much lower in winter with low soil T (< 10 °C). In contrast, the temporal pattern of R_e almost overlapped at different Q_{10} values, and mostly followed the discharge dynamics (black line in Figure 9). Daily R_p varied only slightly (within 15%) with different formations of soil moisture *f*(S_w) (Figure S2B), while R_e almost did not change (Figure 9B). Though we varied Q_{10} from 1.0 to 4.0 in *f(T)*, it is worth noting that varying kinetic rate constant, SOC surface area, volume fraction, and biomass amount could have similar effects (not shown here) because they are all multiplied in Eq. (2).

https://doi.org/10.5194/hess-2019-310
Preprint. Discussion started: 18 July 2019

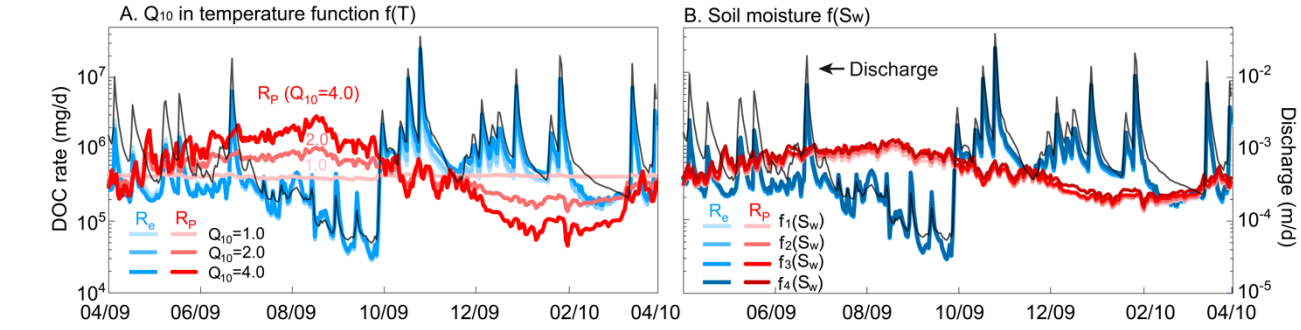

Figure 9. Sensitivity analysis of temporal DOC rates for (A) soil temperature f(T) and (B) soil moisture f(S_w). Varying Q_{10} value in f(T) had a larger influence on R_p than varying f(S_w). Neither f(T) nor f(S_w) had a significant influence on R_e. Instead, R_e mostly followed the temporal trend of discharge, indicating the predominant control of hydrological conditions.

Simulations showed that strong DOC sorption (K_{eq} = 1.0) did not change R_p but lowered stream [DOC] and resulted in smaller R_e (Figure 10A). DOC sorption had little impact on R_e dynamics but increased the magnitude of R_e by 10%-69%. The sorbed [DOC] however differed by more than a factor of 3, with more sorbed DOC with larger K_{eq} values (Figure 10B). High sorbed [DOC] persisted until early fall, when a large rainfall event flushed out the sorbed DOC and reduced the total catchment DOC storage (Figure 6).

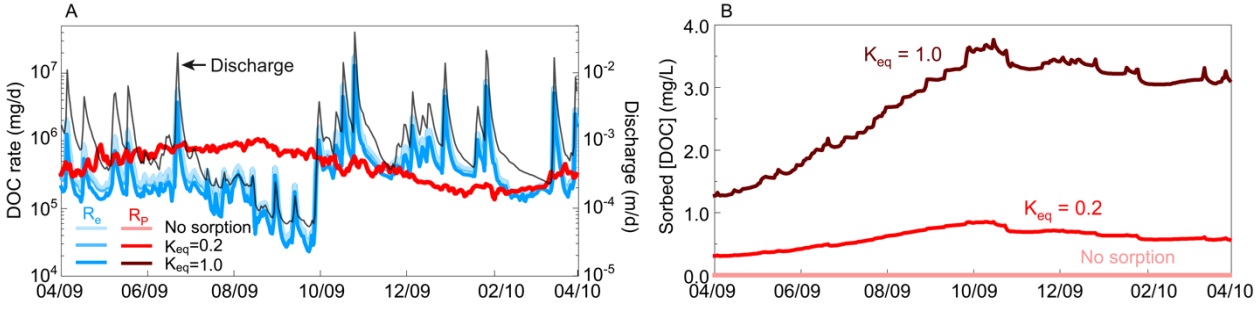

Figure 10. Sensitivity analysis of (A) DOC sorption equilibrium constant K_{eq} on R_p and R_e and (B) the corresponding average [DOC] sorbed on soils at the catchment scale. High K_{eq} led to more DOC sorbed on soils and therefore lower R_e. However, simulated R_e showed similar temporal patterns regardless of K_{eq}.

Varying DOC production characteristics did not change the overall dilution (or chevron) patterns of the DOC C-Q relationship although the magnitude of overall dilution changed slightly in cases with different temperature function *f(T)* and DOC sorption equilibrium constant K_{eq} (Figure 11). High Q_{10} values in *f(T)* led to less dilution, due to more accumulated soil DOC in the dry period (low discharge) and thus more DOC flushing

https://doi.org/10.5194/hess-2019-310
Preprint. Discussion started: 18 July 2019

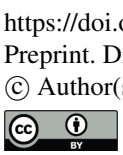

Hydrology and Earth System Sciences
Discussions
Open Access
EGU

with increasing discharge in the dry-to-wet period. High DOC sorption equilibrium constants resulted in more dilution-dominated C-Q relationships as relatively more DOC remained sorbed onto clay minerals under high discharge conditions.

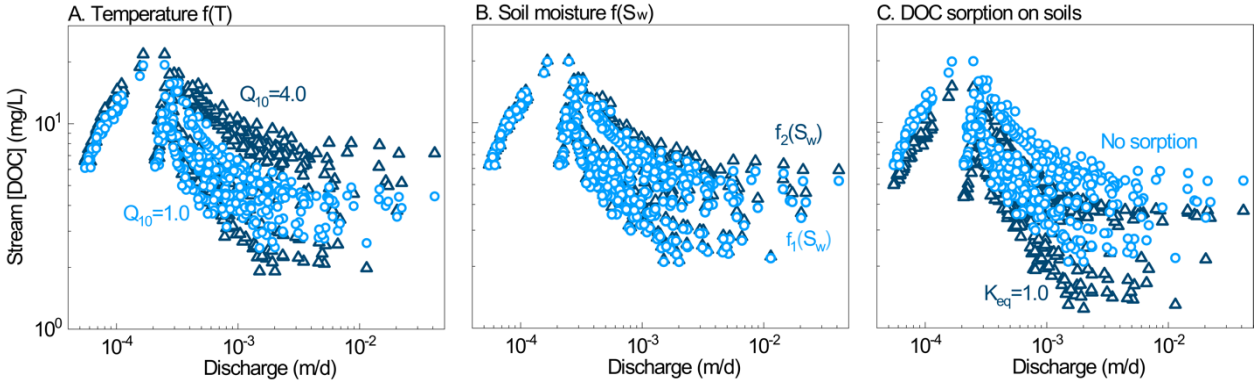

Figure 11. DOC C-Q relationships under different (A) f(T), (B) f(S_w), and (C) DOC sorption equilibrium constants K_{eq}. Only the extreme cases for each scenario are shown. The DOC C-Q relationship was similar in all cases, though the overall dilution pattern slightly changed depending on the different DOC reaction characteristics.

Groundwater control on DOC export. As shown in Figure 12, changing groundwater volume contribution to stream (GW) had more significant impacts on the dynamics of R_e than changing $[DOC]_{GW}$, especially under low discharges ($Q < 1.8\times10^{-4}$ m/d). The increase in the GW contribution from no GW to 2.5GW (i.e. 18.8%) lowered stream [DOC] at low discharges, shifting the C-Q pattern from overall dilution (or chevron pattern) to overall flushing (or flushing until stable). More specifically, the threshold that separated distinct phases of these segmented C-Q responses (Figure 12A2) shifted from $Q = 1.8\times10^{-4}$ m/d to higher discharge values ($\sim 1.0\times10^{-3}$ m/d). This reflects the relative groundwater contribution to streamflow for each case. In contrast, varying $[DOC]_{GW}$ by 2 orders of magnitude while keeping the groundwater contribution (GW) did not change C-Q pattern, because the [DOC] from the swales and valley dominated the stream export.

https://doi.org/10.5194/hess-2019-310
Preprint. Discussion started: 18 July 2019

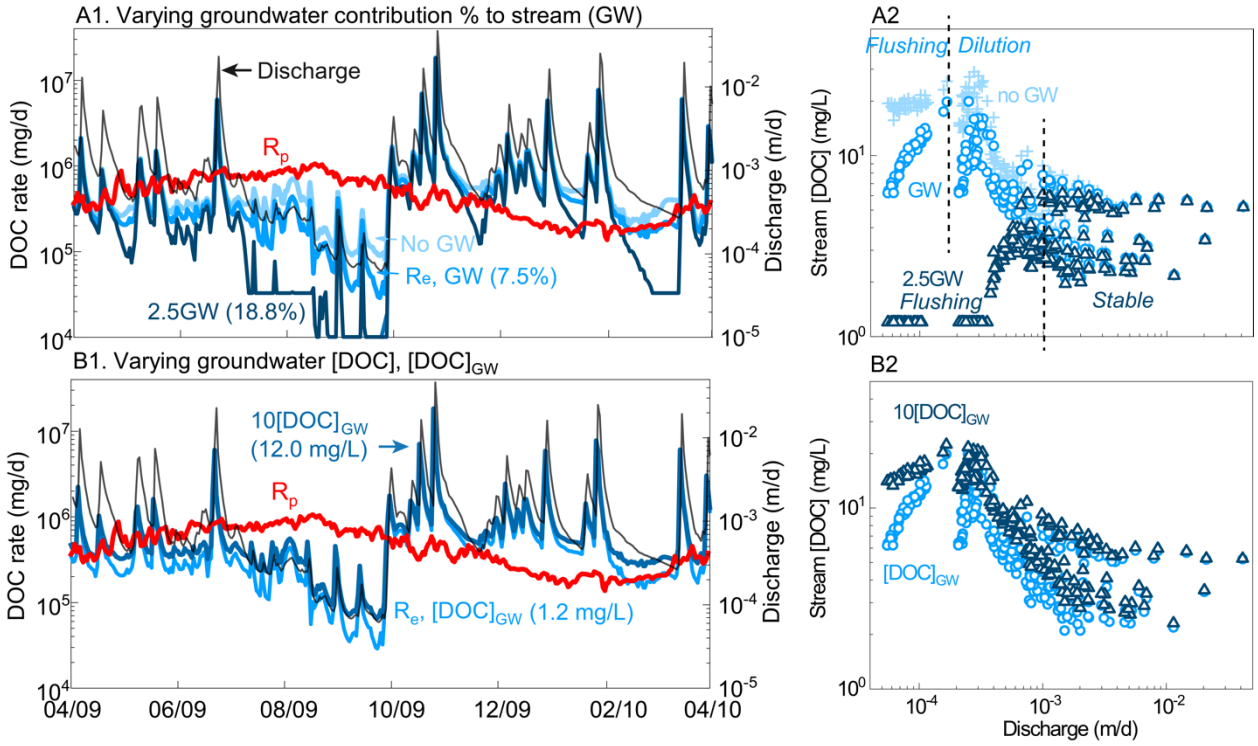

Figure 12. Sensitivity analysis of groundwater on DOC rates (R_p and R_e) and DOC C-Q relationships: (A) scenarios exploring changes in the groundwater volume contribution (%) to stream discharge and (B) scenarios exploring changes in groundwater DOC concentrations $[DOC]_{GW}$. For the base case scenario, $[DOC]_{GW}$ and GW (Q_G/Q) is 1.2 mg/L and 7.5%, respectively. Increases in the relative groundwater contribution to the streamflow lowered R_e and shifted the DOC C-Q pattern from an overall dilution pattern to an overall flushing pattern while changing $[DOC]_{Gw}$ had small influence on DOC rates and C-Q patterns.

Figure 13 summarizes the annual total R_p and R_e at the catchment scale in all sensitivity test scenarios. Annual R_p was most sensitive to T compared to soil moisture and DOC sorption thermodynamics. Higher sensitivity to T (Q_{10} = 4.0) amplified the production and export. However, annual R_e was less sensitive to T variation though it also increased with Q_{10} because a higher production of DOC R_p change led to more export of DOC. Annual R_p also depended on $f(S_w)$ with a threshold function $f_4(S_w)$ (Section 2.6) having the highest production rates. However, annual R_e did not follow the trend of R_p (Figure 13B). Generally, under the same hydrological conditions, the doubling of annual R_p only led to about 50% increase in R_e. Higher sorption capacity (higher K_{eq}) did not change production rates but could reduce DOC export by about 30%, because large amount of DOC could be stored in the catchment. High relative groundwater inputs (18.8% versus 7.5%) lowered R_e in all scenarios because more water came from deeper groundwater containing a lower DOC level.

https://doi.org/10.5194/hess-2019-310
Preprint. Discussion started: 18 July 2019

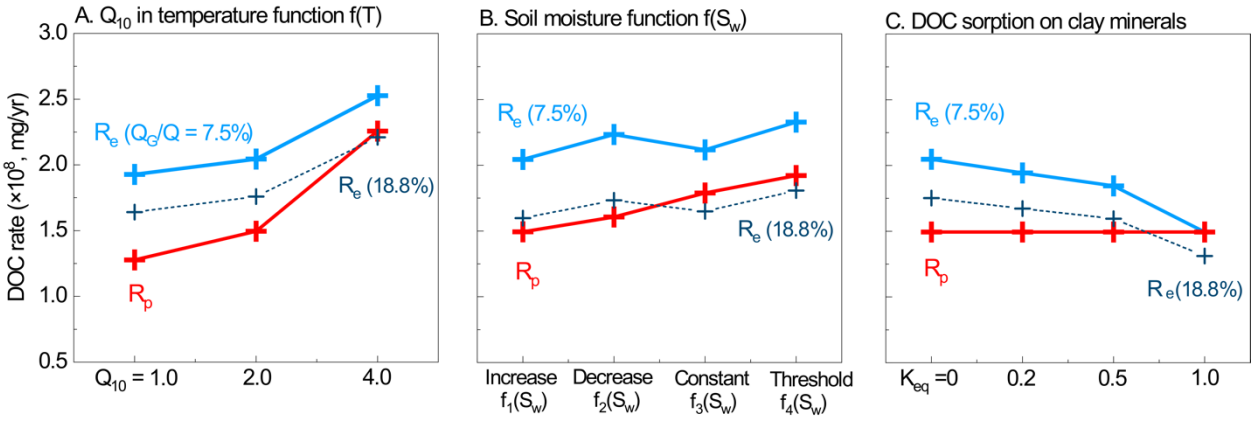

Figure 13. Total R_p (red) and R_e (blue) per year (mg/yr) under different groundwater influxes, including 7.5% and 18.8% groundwater volume contribution to the streamflow. Three different scenarios were considered: (A) soil *T*, (B) soil moisture, and (C) DOC sorption equilibrium constant K_{eq}. Each symbol represents the total value from each simulation (one-year cycle). The sensitivity of R_e to environmental factors was lower than that of R_p. As groundwater in this work flows below the soil-weathered rock interface, changing groundwater contribution to the stream does not change the DOC biogeochemical processes. Thus, R_p was identified for both groundwater contribution level while R_e decreased with increasing groundwater contribution.

4. Discussion

Using a reactive-transport model applied to a humid temperate first-order catchment drained by an intermittent stream, we found contrasting temporal dynamics and environmental controls of DOC production and export. Our study revealed that DOC production was primarily determined by temperature, but that lateral export of DOC was most sensitive to changes in hydrology. This work contributes to the growing body of research that lateral carbon flux is primarily determined by water routing and hydrological connectivity and only secondarily influenced by biological activity (Zarnetske et al., 2018).

DOC production. Simulated catchment-scale DOC production rate R_p depends more on *T* than water storage or soil moisture. This finding is expected, as DOC production is biologically mediated and thus, influenced by temperature via the metabolism of plants and microbes (Gillooly et al., 2001). Moreover, soil moisture is relatively constant in this temperate humid catchment (from 0.46 to 0.56), especially compared to other forested catchments where water availability is more limited and soil moisture can drop below 0.15 (Korres et al., 2015).

https://doi.org/10.5194/hess-2019-310
Preprint. Discussion started: 18 July 2019


Hydrology and Earth System Sciences
Discussions

The influence of soil moisture on R_p would likely be higher in catchments with more pronounced seasonal changes in soil moisture.

Our work also suggests that catchment-scale (R_P) and local-scale (r_P) production rates have different primary controls. The rate law used for DOC production at the local scale is measured at relatively small spatial scales (0.1-2.0 m in soil pedons) (Bauer et al., 2008; Hongve, 1999; Yan et al., 2016). Our results show that even when the rate law with an optimum soil moisture was used at the local scale ($f_4(S_w)$ in Figure S2B), the catchment-scale rates do not exhibit maximum rates at an "optimal" soil moisture (Figure 8), indicating different controls on production rates at the local versus catchment scale. On the other hand, due to spatial heterogeneities of T, soil moisture and SOC content, the temporal variations of R_P and r_P may be not consistent. At Shale Hills, the daily R_p spans less than an order of magnitude, with its maximum occurring in the dry, hot summer and minimum at wet, cold winter and spring (Figure 6). Local-scale r_p exhibits similar temporal dynamics but varied by more than 2 orders of magnitude, with rapid production mostly in "hot spots", i.e., swales and riparian zones with persistently higher water and SOC content than the rest of the domain (Figure 5). Note that local scale rate laws are often extrapolated directly to catchments or larger scales (Crowther et al., 2016; Conant et al., 2011; Fissore et al., 2009; Moyano et al., 2012). Our work suggests that this could lead to large uncertainties in upscaling of carbon fluxes.

DOC lateral export. In contrast to DOC production, simulated DOC export rate R_e is largely driven by outflow and soil water [DOC] in the temporally-variable, hydrologically connected zones. The [DOC] measured at the catchment outflow therefore primarily reflects an integration of those within the connected zones. The temporal and spatial balance of connected zones is, in turn, highly dependent on the catchment size, hydrogeologic structure, vegetation, boundary conditions and climatic setting. Geomorphological and ecological processes have been shown to co-create systematic differences in the vertical and lateral distribution of SOC and living plant biomass, with greater concentrations of organic carbon in valley floor than in hillslopes (Piney et al., 2018; Temnerud et al., 2016; Campeau et al., 2019; Thomas et al., 2016). This pattern of SOC distribution may help explain the large variation of stream [DOC] in catchments within similar climate zones but with different hydrological conditions (Moatar et al., 2017). For example, the median stream [DOC] at Shale Hills is relatively high (10.0 mg/L), compared to 3.0 mg/L in temperate humid German catchments (Musolff et al., 2018), 4.1 mg/L in the UK catchments with oceanic climate (Monteith et al., 2015), 4.50 mg/L in France (Moatar et al., 2017), but similar to 9.5 mg/L measured in boreal catchments in Sweden (Winterdahl et al., 2014), 8.1 mg/L in boreal wet and 10.5 mg/L in boreal dry sites in Norway and Finland (de Wit et al., 2016). These differences suggest that hydrological processes and landscape heterogeneity as moderating determinants of the degree of hydrological connectivity within catchments may be more important drivers of the catchment-scale DOC export than climate.

https://doi.org/10.5194/hess-2019-310
Preprint. Discussion started: 18 July 2019


Hydrology and Earth System Sciences
Discussions

Temporal asynchrony of DOC production and export. The contrasting temporal pattern of simulated DOC production and export reflects the asynchronous nature of these two processes at the catchment scale. The local DOC production is influenced mostly by the seasonal pattern of soil *T* that determined the local storage of DOC while its export is predominantly controlled by the precipitation event-driven water fluxes, antecedent conditions and degree of hydrological connection of DOC production zones to the stream. The temporal asynchrony between DOC production and export rates is therefore strongly influenced by the seasonality of hydrological connectivity. During wet conditions (winter and spring), the catchment is well-connected and there are small differences between the rate of DOC production and export. During dry conditions (summer), DOC production rates can be orders of magnitude higher than the export rates. The catchment essentially stores the produced DOC in soil water and on soil surfaces, leading to the continued accumulation of DOC until the next precipitation events arrive and flush out the stored DOC. Hence, low hydrological connectivity implies a delay in DOC export such that the DOC we see today in the stream may be often the DOC produced a while ago. Moreover, our simulations suggest that DOC storage depends not only on hydrological connectivity, but also on the sorbing capacity of the soils. In this context, clay content and the presence of organo-mineral aggregates might play a role in mediating DOC dynamics (Lehmann et al., 2007; Cincotta et al.). These findings echo the observations that antecedent moisture conditions are essential for understanding the temporal pattern of DOC export, especially in forested catchments in water limited regions (Bernal et al. 2002), and previous studies showing that hydrological connectivity and water flow paths become dominant as subsurface saturation expands across valley floors and into hillslopes (Covino, 2017; Abbott et al., 2016a). In contrast, our results differ from existing studies at soil pedons showing the synchronization of DOC production and export rates (Michalzik et al., 2001). These differences are likely due to the relatively short water residence time and well-connected systems at the pedon scale.

The asynchronous nature of DOC production and export has important implications for the proportional role of lateral carbon fluxes in different ecosystems. In less hydrologically connected ecosystems, DOC export will be dominated by high flow events, when biogeochemical production mechanisms exert little to no influence. In more hydrologically connected ecosystems, DOC export will occur throughout the year, including low-flow periods when biogeochemical processes could modulate DOC flux.

Regulation of C-Q patterns. As in many small catchments, hydrological connectivity primarily occurs in the riparian zone and swales (analogy to wetlands) with high SOC and water content. During the dry period, the connected zone is restricted to soils of the valley floor characterized by high SOC rates and soil water [DOC] (Figure 5 and Figure 7), and the high stream [DOC] is sourced from by the lateral flux through these valley floor soils. Stream [DOC] increases with the expanding connected zones until reaching a threshold connectivity value

https://doi.org/10.5194/hess-2019-310
Preprint. Discussion started: 18 July 2019


Hydrology and Earth System Sciences
Discussions

(~0.1 ≈ the valley width / the catchment width) of hydrological connectivity. Upon reaching this threshold, an increasing relative contribution of lateral flow from planar hillslopes and uplands characterized by low soil water [DOC] increased sharply and the stream [DOC] dropped, leading to an emergent dilution C-Q pattern. In other words, during wet periods when the whole catchment is hydrologically connected to the stream, stream [DOC] reflects the "average" concentration across the catchment (~ 2.5 mg/L). At dry times, however, only the DOC at the very vicinity of the catchment (with high SOC content) shows up in the stream. The increase and then decrease pattern (or chevron pattern) may indicate the presence of three members in determining the C-Q patterns: the groundwater with very low DOC concentration, the soil water in organic-rich swales with high DOC content, and the uphill soil water with DOC level in between these two.

The overall dilution (or chevron) C-Q pattern observed here with a maximum at a mid-range discharge contrasts the most commonly observed flushing pattern for DOC (Moatar et al., 2017). In fact, it resembles more of the hysteresis behavior often observed in storm and snowmelt events for metals and nutrients (Zhi et al., 2019; Duncan et al., 2017). Previous field studies illustrate that the hydrological connectivity to the stream versus the distribution of SOC ultimately dictates the spatial and temporal dynamics of DOC in soil and stream water, leading to different C-Q relationships (dilution versus flushing) (Bernhardt et al., 2017; Bernal and Sabater, 2012; Covino, 2017). This tradeoff is illustrated by different C-Q relationships in two head-catchments Shale Hills (US) and Plynlimon (UK) (Herndon et al., 2015). Stream water at Shale Hills is derived from SOC-rich swales with high [DOC] at low flow and from both swales and hillslopes with low [DOC] when discharge increases. Conversely, at Plynlimon, SOC is enriched in uplands and therefore concentrations are high at high flow when water flows connect SOC-rich uplands. Our reactive transport modeling provides a quantitative and mechanistic approach to explain the overall dilution behavior of C-Q patterns, which have usually been interpreted as a production/source limitation (Zarnetske et al., 2018; Covino, 2017). Our results are consisted with Covino (2017) proposed mechanisms on driving forces: solute concentrations could increase with connectivity first due to transport limitation while they may decrease with connectivity after a given threshold due to reactivity limitation. Here based on the model, the source limitation essentially means solutes that are enriched in a limited zone within the catchment. Together, these studies suggest that C-Q patterns emerge from a combination of different hydrological and biogeochemical processes, and thus may be much more complicated than initially thought. Modelling approaches such as the one presented here can help us to understand the mechanisms underlying C-Q patterns, and thus improve our ability to predict the evolution of C-Q trajectories under changing climatic conditions.

C-Q patterns also relate to the mixture of different sources of water in the stream, composed of time-varying relative contribution from the shallow soil water and relatively deep groundwater. Their DOC relative

https://doi.org/10.5194/hess-2019-310
Preprint. Discussion started: 18 July 2019


Hydrology and Earth System Sciences
Discussions

contribution can be affected by the vertical distribution of reacting materials (Musolff et al., 2017; Bishop et al., 2004; Seibert et al., 2009; Winterdahl et al., 2016) and the relative volume contribution of source water (soil water vs groundwater below the soil-weathered rock interface) to the stream (Zhi et al., 2019; Radke et al., 2019; Weigand et al., 2017). With the shale bedrock, the groundwater contribution to the stream is relatively small (~7.5%) at Shale Hills. Soil water (although from a very limited swale area) dominates inflow to the stream even during the summer dry period. When the groundwater volume input is increased to about 18.8% of the streamflow by volume (2.5× the actual case), as shown in the sensitivity analysis (Figure 12), the C-Q relationships shift to an overall flushing pattern. This may provide a potential explanation for the DOC C-Q flushing pattern at sandstone-dominant Garner Run (a neighbor catchment of Shale Hills), where the groundwater contributions to the stream are typically higher (Hoagland et al., 2017; Li et al., 2018). More interestingly, this indicates when the groundwater contribution is "sufficiently" high, it might mask the signature of the swale-derived soil water such that the three end-member chevron C-Q pattern become a two end-member pattern with monotonic flushing behavior as observed in Coal Creek where groundwater contributes about 20% annually (Zhi et al., 2019). C-Q relationships have been categorized into 9 patterns, including 3 monotonic and 9 segmented types (Moatar et al., 2017; Underwood et al., 2017). The shifting threshold that separates segments of C-Q responses with the relative groundwater contribution in this work (Figure 12) suggests the relative contribution of groundwater to streamflow may play a pivotal role in shaping the C-Q patterns. And this threshold value may provide a rough estimation for the relative contribution of different end-members to the stream.

Implications for CO_2 production and vertical carbon fluxes. Although not explicitly simulated in this work, the potential removal of DOC via respiration into CO_2 are also microbially mediated. In hence, the drivers for DOC dynamics in catchment soils may also affect the CO_2 production and vertical carbon fluxes. Generally, warm temperatures and medium soil moisture provide ideal conditions for microbial respiration, leading to significant vertical losses of carbon during summer months (Perdrial et al., 2018; Stielstra et al., 2015). The high stored DOC mass in summer at Shale Hills provides enough source for microbial and therefore enhance vertical carbon losses. However, this high DOC accumulation also indicates that DOC production may be dominant over the vertical loss via CO_2. In contrast, low temperatures and very high soil moisture can hinder aerobic respiration and associated carbon losses as CO_2 (Smith et al., 2003), effectively accumulating carbon until hydrologic flushing transfers DOC to streams (Pacific et al., 2010). The annual DOC export rate of 2.0 g/m^2/yr at Shale Hills is comparable to those (2.0-5.0 g/m^2/yr) in large tropical river systems (e.g. Amazon and Mekong) with high *T* and discharge (Li et al., 2019). This is probably because the short water and solute residence time in small catchments lowers the vertical loss of DOC into CO_2.

https://doi.org/10.5194/hess-2019-310
Preprint. Discussion started: 18 July 2019


Hydrology and Earth System Sciences
Discussions

5. Conclusions

The production and export of DOC remain central uncertainties in determining ecosystem-level carbon balance (Raymond et al., 2016; Catalan et al., 2016; Kicklighter et al., 2013). These uncertainties persist despite many studies because there are complex interacting controls on DOC production and export. Indeed, very few studies have quantitatively addressed the linkages between SOC processing, hydrological conditions, and corresponding DOC processing and export rates at the catchment scale. We found that DOC production was the major DOC source at Shale Hills (76%, compared to 24% from precipitation). Our simulations showed that the temporal dynamics of DOC export rates (R_e) were more linked to hydrological flow paths and precipitation events than to production rates (R_p). Sensitivity analysis further confirmed that R_p was primarily controlled by temperature while R_e was most sensitive to changes in hydrology. This difference in environmental drivers lead to an asynchrony between DOC production and DOC export which was amplified as the summer drought proceeds. During the wet period (spring and winter), the catchment was well connected and DOC production and export occurred simultaneously, while during summer, DOC accumulated in soil pockets disconnected from the stream, and DOC export was limited and constrained to the near stream areas.

This work quantitatively demonstrates the key role of hydrological flow paths and the degree of connectivity in determining the C-Q patterns exhibited at the catchment outlet. At low discharges where connectivity is limited (<0.1), stream DOC was mainly sourced from the valley floor which maintained high SOC decomposition rates and soil water [DOC]. At higher discharges, an increasing relative contribution of soil lateral flow from planar hillslopes and uplands characterized by low soil water [DOC], decreasing the stream [DOC] and therefore exhibiting a dilution C-Q pattern. Although changing the effect of soil *T*, moisture, and sorption on DOC reaction characteristics alters soil water [DOC], there is little change in the overall C-Q patterns. However, when groundwater contributes 18.8% of total annual discharge, stream [DOC] increases with discharge and flushing patterns emerge, emphasizing the significance of relative contribution from different water sources in shaping DOC export behaviors. This study provides new insights into how DOC production and export interact at multiple scales, and emphasizes the importance of considering different constraints when projecting the response of lateral and vertical carbon fluxes to climate changes.

https://doi.org/10.5194/hess-2019-310
Preprint. Discussion started: 18 July 2019


Hydrology and Earth System Sciences
Discussions

Author contributions. HW, LL, and all other co-authors initiated the idea via a workshop and monthly discussions, HW and LL designed the numerical experiments, HW ran the simulations, analyzed simulation results, and wrote the first draft of the manuscript. All co-authors participated in editing the manuscript.

Competing interests. The authors report no conflicts of interest.

Acknowledgements. We acknowledge the financial support from the US National Science Foundation Geobiology and Low temperature Geochemistry program via the grant EAR-1724171. We thank the ISU Center for Ecological Research and Education and EPSCoR grant IIA 1301792 that stimulated ideas in this manuscript.

References

Abbott, B. W., Jones, J. B., Godsey, S. E., Larouche, J. R., and Bowden, W. B.: Patterns and persistence of hydrologic carbon and nutrient export from collapsing upland permafrost, Biogeosciences, 12, 3725-3740, 10.5194/bg-12-3725-2015, 2015.

Abbott, B. W., Baranov, V., Mendoza-Lera, C., Nikolakopoulou, M., Harjung, A., Kolbe, T., Balasubramanian, M. N., Vaessen, T. N., Ciocca, F., Campeau, A., Wallin, M. B., Romeijn, P., Antonelli, M., Goncalves, J., Datry, T., Laverman, A. M., de Dreuzy, J. R., Hannah, D. M., Krause, S., Oldham, C., and Pinay, G.: Using multi-tracer inference to move beyond single-catchment ecohydrology, Earth-Sci Rev, 160, 19-42, 10.1016/j.earscirev.2016.06.014, 2016a.

Abbott, B. W., Jones, J. B., Schuur, E. A. G., Chapin, F. S., Bowden, W. B., Bret-Harte, M. S., Epstein, H. E., Flannigan, M. D., Harms, T. K., Hollingsworth, T. N., Mack, M. C., McGuire, A. D., Natali, S. M., Rocha, A. V., Tank, S. E., Turetsky, M. R., Vonk, J. E., Wickland, K. P., Aiken, G. R., Alexander, H. D., Amon, R. M. W., Benscoter, B. W., Bergeron, Y., Bishop, K., Blarquez, O., Bond-Lamberty, B., Breen, A. L., Buffam, I., Cai, Y. H., Carcaillet, C., Carey, S. K., Chen, J. M., Chen, H. Y. H., Christensen, T. R., Cooper, L. W., Cornelissen, J. H. C., de Groot, W. J., DeLuca, T. H., Dorrepaal, E., Fetcher, N., Finlay, J. C., Forbes, B. C., French, N. H. F., Gauthier, S., Girardin, M. P., Goetz, S. J., Goldammer, J. G., Gough, L., Grogan, P., Guo, L. D., Higuera, P. E., Hinzman, L., Hu, F. S., Hugelius, G., Jafarov, E. E., Jandt, R., Johnstone, J. F., Karlsson, J., Kasischke, E. S., Kattner, G., Kelly, R., Keuper, F., Kling, G. W., Kortelainen, P., Kouki, J., Kuhry, P., Laudon, H., Laurion, I., Macdonald, R. W., Mann, P. J., Martikainen, P. J., McClelland, J. W., Molau, U., Oberbauer, S. F., Olefeldt, D., Pare, D., Parisien, M. A., Payette, S., Peng, C. H., Pokrovsky, O. S., Rastetter, E. B., Raymond, P. A., Raynolds, M. K., Rein, G., Reynolds, J. F., Robards, M., Rogers, B. M., Schadel, C., Schaefer, K., Schmidt, I. K., Shvidenko, A., Sky, J., Spencer, R. G. M., Starr, G., Striegl, R. G., Teisserenc, R., Tranvik, L. J., Virtanen, T., Welker, J. M., and Zimov, S.: Biomass offsets little or none of permafrost carbon release from soils, streams, and wildfire: an expert assessment, Environmental Research Letters, 11, 10.1088/1748-9326/11/3/034014, 2016b.

https://doi.org/10.5194/hess-2019-310
Preprint. Discussion started: 18 July 2019

Allard, D.: Simulating a geological lithofacies with respect to connectivity information using the truncated gaussian model, Geostatistical Simulations: Proceedings of the Geostatistical Simulation Workshop, edited by:
Armstrong, M., and Dowd, P. A., 197-211 pp., 1994.
Andrews, D. M., Lin, H., Zhu, Q., Jin, L. X., and Brantley, S. L.: Hot Spots and Hot Moments of Dissolved Organic Carbon Export and Soil Organic Carbon Storage in the Shale Hills Catchment, Vadose Zone J, 10, 943-954, 10.2136/vzj2010.0149, 2011.
Aufdenkampe, A. K., Mayorga, E., Raymond, P. A., Melack, J. M., Doney, S. C., Alin, S. R., Aalto, R. E., and Yoo, K.: Riverine coupling of biogeochemical cycles between land, oceans, and atmosphere, Front. Ecol. Environ., 9, 53-60, 10.1890/100014, 2011.
Bao, C., Li, L., Shi, Y. N., and Duffy, C.: Understanding watershed hydrogeochemistry: 1. Development of RT-Flux-PIHM, Water Resour Res, 53, 2328-2345, 10.1002/2016wr018934, 2017.
Battin, T. J., Luyssaert, S., Kaplan, L. A., Aufdenkampe, A. K., Richter, A., and Tranvik, L. J.: The boundless carbon cycle, Nature Geoscience, 2, 598-600, 10.1038/ngeo618, 2009.
Bauer, J., Herbst, M., Huisman, J. A., Weihermuller, L., and Vereecken, H.: Sensitivity of simulated soil heterotrophic respiration to temperature and moisture reduction functions, Geoderma, 145, 17-27, 10.1016/j.geoderma.2008.01.026, 2008.
Bernal, S., Butturini, A., and Sabater, F.: Variability of DOC and nitrate responses to storms in a small Mediterranean forested catchment, Hydrol Earth Syst Sc, 6, 1031-1041, 10.5194/hess-6-1031-2002, 2002.
Bernal, S., and Sabater, F.: Changes in discharge and solute dynamics between hillslope and valley-bottom intermittent streams, Hydrol Earth Syst Sc, 16, 1595-1605, 10.5194/hess-16-1595-2012, 2012.
Bernhardt, E. S., Blaszczak, J. R., Ficken, C. D., Fork, M. L., Kaiser, K. E., and Seybold, E. C.: Control Points in Ecosystems: Moving Beyond the Hot Spot Hot Moment Concept, Ecosystems, 20, 665-682, 10.1007/s10021-016-0103-y, 2017.
Billings, S. A., Hirmas, D., Sullivan, P.L., Lehmeier, C.A., Bagchi, S., Min, K., Brecheisen, Z., Hauser, E., Stair, R., Flournoy, R. and Richter, D. deB . Loss of deep roots limits biogenic agents of soil development that are only partially restored by decades of forest regeneration, Elem Sci Anth, 6, 34, 10.1525/elementa.287, 2018.
Bishop, K., Seibert, J., Köhler, S., and Laudon, H.: Resolving the Double Paradox of rapidly mobilized old water with highly variable responses in runoff chemistry, Hydrol. Process., 18, 185-189, doi:10.1002/hyp.5209, 2004.
Bolan, N. S., Adriano, D. C., Kunhikrishnan, A., James, T., McDowell, R., and Senesi, N.: Dissolved organic matter: biogeochemistry, dynamics, and environmental significance in soils, in: Advances in Agronomy, Vol 110, edited by: Sparks, D. L., Advances in Agronomy, Elsevier Academic Press Inc, San Diego, 1-75, 2011.
Brooks, P. D., McKnight, D. M., and Bencala, K. E.: The relationship between soil heterotrophic activity, soil dissolved organic carbon (DOC) leachate, and catchment-scale DOC export in headwater catchments, Water Resour Res, 35, 1895-1902, 10.1029/1998wr900125, 1999.
Campeau, A., Bishop, K., Amvrosiadi, N., Billett, M. F., Garnett, M. N., Laudon, H., Oquist, M. G., and Wallin, M. B.: Current forest carbon fixation fuels stream CO2 emissions, Nature Communications, 10, 10.1038/s41467-019-09922-3, 2019.
Catalan, N., Marce, R., Kothawala, D. N., and Tranvik, L. J.: Organic carbon decomposition rates controlled by water retention time across inland waters, Nature Geoscience, 9, 501-+, 10.1038/ngeo2720, 2016.
Chapin, F. S., Woodwell, G. M., Randerson, J. T., Rastetter, E. B., Lovett, G. M., Baldocchi, D. D., Clark, D. A., Harmon, M. E., Schimel, D. S., Valentini, R., Wirth, C., Aber, J. D., Cole, J. J., Goulden, M. L., Harden, J. W., Heimann, M., Howarth, R. W., Matson, P. A., McGuire, A. D., Melillo, J. M., Mooney, H. A., Neff, J. C., Houghton, R. A., Pace, M. L., Ryan, M. G., Running, S. W., Sala, O. E., Schlesinger, W. H., and Schulze, E. D.: Reconciling carbon-cycle concepts, terminology, and methods, Ecosystems, 9, 1041-1050, 10.1007/s10021-005-0105-7, 2006.

https://doi.org/10.5194/hess-2019-310
Preprint. Discussion started: 18 July 2019

Cincotta, M., Perdrial, J. N., Shavitz, A., Shanley, J., Perdrial, N., Armfield, J., Liebenson, A., Landsman, M., and Adler, T.: Soil aggregates as source of dissolved organic carbon to streams: an experimental study on the effect of solution chemistry on water extractable carbon, Frontiers in Earth Science: Biogeosciences, 2019.

Clark, J. M., Bottrell, S. H., Evans, C. D., Monteith, D. T., Bartlett, R., Rose, R., Newton, R. J., and Chapman, P. J.: The importance of the relationship between scale and process in understanding long-term DOC dynamics, Science of the Total Environment, 408, 2768-2775, 10.1016/j.scitotenv.2010.02.046, 2010.

Conant, R. T., Ryan, M. G., Agren, G. I., Birge, H. E., Davidson, E. A., Eliasson, P. E., Evans, S. E., Frey, S. D., Giardina, C. P., Hopkins, F. M., Hyvonen, R., Kirschbaum, M. U. F., Lavallee, J. M., Leifeld, J., Parton, W. J., Steinweg, J. M., Wallenstein, M. D., Wetterstedt, J. A. M., and Bradford, M. A.: Temperature and soil organic matter decomposition rates - synthesis of current knowledge and a way forward, Glob. Change Biol., 17, 3392-3404, 10.1111/j.1365-2486.2011.02496.x, 2011.

Covino, T.: Hydrologic connectivity as a framework for understanding biogeochemical flux through watersheds and along fluvial networks, Geomorphology, 277, 133-144, 10.1016/j.geomorph.2016.09.030, 2017.

Crowther, T. W., Todd-Brown, K. E. O., Rowe, C. W., Wieder, W. R., Carey, J. C., Machmuller, M. B., Snoek, B. L., Fang, S., Zhou, G., Allison, S. D., Blair, J. M., Bridgham, S. D., Burton, A. J., Carrillo, Y., Reich, P. B., Clark, J. S., Classen, A. T., Dijkstra, F. A., Elberling, B., Emmett, B. A., Estiarte, M., Frey, S. D., Guo, J., Harte, J., Jiang, L., Johnson, B. R., Kroel-Dulay, G., Larsen, K. S., Laudon, H., Lavallee, J. M., Luo, Y., Lupascu, M., Ma, L. N., Marhan, S., Michelsen, A., Mohan, J., Niu, S., Pendall, E., Penuelas, J., Pfeifer-Meister, L., Poll, C., Reinsch, S., Reynolds, L. L., Schmidt, I. K., Sistla, S., Sokol, N. W., Templer, P. H., Treseder, K. K., Welker, J. M., and Bradford, M. A.: Quantifying global soil carbon losses in response to warming, Nature, 540, 104-+, 10.1038/nature20150, 2016.

D'Amore, D. V., Edwards, R. T., Herendeen, P. A., Hood, E., and Fellman, J. B.: Dissolved Organic Carbon Fluxes from Hydropedologic Units in Alaskan Coastal Temperate Rainforest Watersheds, Soil Science Society of America Journal, 79, 378-388, 10.2136/sssaj2014.09.0380, 2015.

Davidson, E. A., and Janssens, I. A.: Temperature sensitivity of soil carbon decomposition and feedbacks to climate change, Nature, 440, 165-173, 10.1038/nature04514, 2006.

de Wit, H. A., Ledesma, J. L. J., and Futter, M. N.: Aquatic DOC export from subarctic Atlantic blanket bog in Norway is controlled by seasalt deposition, temperature and precipitation, Biogeochemistry, 127, 305-321, 10.1007/s10533-016-0182-z, 2016.

Duffy, C., Shi, Y., Davis, K., Slingerland, R., Li, L., Sullivan, P. L., Goddéris, Y., Brantley, S. L. J. P. E., and Science, P.: Designing a suite of models to explore critical zone function, 10, 7-15, 2014.

Duncan, J. M., Welty, C., Kemper, J. T., Groffman, P. M., and Band, L. E.: Dynamics of nitrate concentration-discharge patterns in an urban watershed, Water Resour. Res., 53, 7349-7365, doi:10.1002/2017WR020500, 2017.

Evans, C. D., Monteith, D. T., and Cooper, D. M.: Long-term increases in surface water dissolved organic carbon: Observations, possible causes and environmental impacts, Environ. Pollut., 137, 55-71, 10.1016/j.envpol.2004.12.031, 2005.

Evans, C. D., Jones, T. G., Burden, A., Ostle, N., Zielinski, P., Cooper, M. D. A., Peacock, M., Clark, J. M., Oulehle, F., Cooper, D., and Freeman, C.: Acidity controls on dissolved organic carbon mobility in organic soils, Glob. Change Biol., 18, 3317-3331, 10.1111/j.1365-2486.2012.02794.x, 2012.

Fissore, C., Giardina, C. P., Kolka, R. K., and Trettin, C. C.: Soil organic carbon quality in forested mineral wetlands at different mean annual temperature, Soil Biology & Biochemistry, 41, 458-466, 10.1016/j.soilbio.2008.11.004, 2009.

Gillooly, J. F., Brown, J. H., West, G. B., Savage, V. M., and Charnov, E. L.: Effects of size and temperature on metabolic rate, Science, 293, 2248-2251, 10.1126/science.1061967, 2001.

Godsey, S. E., Kirchner, J. W., and Clow, D. W.: Concentration-discharge relationships reflect chemostatic characteristics of US catchments, Hydrological Processes, 23, 1844-1864, 10.1002/hyp.7315, 2009.

Hale, R. L., Turnbull, L., Earl, S. R., Childers, D. L., and Grimm, N. B.: Stormwater Infrastructure Controls Runoff and Dissolved Material Export from Arid Urban Watersheds, Ecosystems, 18, 62-75, 10.1007/s10021-014-9812-2, 2015.

Herndon, E. M., Dere, A. L., Sullivan, P. L., Norris, D., Reynolds, B., and Brantley, S. L.: Landscape heterogeneity drives contrasting concentration-discharge relationships in shale headwater catchments, Hydrol Earth Syst Sc, 19, 3333-3347, 10.5194/hess-19-3333-2015, 2015.

Hoagland, B., Russo, T. A., Gu, X., Hill, L., Kaye, J., Forsythe, B., and Brantley, S. L.: Hyporheic zone influences on concentration-discharge relationships in a headwater sandstone stream, Water Resour Res, 53, 4643-4667, 10.1002/2016wr019717, 2017.

Hongve, D.: Production of dissolved organic carbon in forested catchments, J Hydrol, 224, 91-99, 10.1016/s0022-1694(99)00132-8, 1999.

Hugelius, G., Strauss, J., Zubrzycki, S., Harden, J. W., Schuur, E. A. G., Ping, C. L., Schirrmeister, L., Grosse, G., Michaelson, G. J., Koven, C. D., O'Donnell, J. A., Elberling, B., Mishra, U., Camill, P., Yu, Z., Palmtag, J., and Kuhry, P.: Estimated stocks of circumpolar permafrost carbon with quantified uncertainty ranges and identified data gaps, Biogeosciences, 11, 6573-6593, 10.5194/bg-11-6573-2014, 2014.

Humbert, G., Jaffrezic, A., Fovet, O., Gruau, G., and Durand, P.: Dry-season length and runoff control annual variability in stream DOC dynamics in a small, shallow groundwater-dominated agricultural watershed, Water Resour Res, 51, 7860-7877, 10.1002/2015wr017336, 2015.

Iavorivska, L., Boyer, E. W., Miller, M. P., Brown, M. G., Vasilopoulos, T., Fuentes, J. D., and Duffy, C. J.: Atmospheric inputs of organic matter to a forested watershed: Variations from storm to storm over the seasons, Atmospheric Environment, 147, 284-295, 10.1016/j.atmosenv.2016.10.002, 2016.

Jarvis, P., and Linder, S.: Botany - Constraints to growth of boreal forests, Nature, 405, 904-905, 10.1038/35016154, 2000.

Jennings, E., Jarvinen, M., Allott, N., Arvola, L., Moore, K., Naden, P., Aonghusa, C. N., Noges, T., and Weyhenmeyer, G. A.: Impacts of Climate on the Flux of Dissolved Organic Carbon from Catchments, in: Impact of Climate Change on European Lakes, edited by: George, G., Aquatic Ecology Series, Springer, Dordrecht, 199-220, 2010.

Jin, L., and Brantley, S. L.: Soil chemistry and shale weathering on a hillslope influenced by convergent hydrologic flow regime at the Susquehanna/Shale Hills Critical Zone Observatory, Applied Geochemistry, 26, Supplement, S51-S56, 10.1016/j.apgeochem.2011.03.027, 2011.

Jin, L. X., Ravella, R., Ketchum, B., Bierman, P. R., Heaney, P., White, T., and Brantley, S. L.: Mineral weathering and elemental transport during hillslope evolution at the Susquehanna/Shale Hills Critical Zone Observatory, Geochim Cosmochim Ac, 74, 3669-3691, 10.1016/j.gca.2010.03.036, 2010.

Kicklighter, D. W., Hayes, D. J., McClelland, J. W., Peterson, B. J., McGuire, A. D., and Melillo, J. M.: Insights and issues with simulating terrestrial DOC loading of Arctic river networks, Ecological Applications, 23, 1817-1836, 10.1890/11-1050.1, 2013.

Korres, W., Reichenau, T. G., Fiener, P., Koyama, C. N., Bogena, H. R., Comelissen, T., Baatz, R., Herbst, M., Diekkruger, B., Vereecken, H., and Schneider, K.: Spatio-temporal soil moisture patterns - A meta-analysis using plot to catchment scale data, J Hydrol, 520, 326-341, 10.1016/j.jhydrol.2014.11.042, 2015.

Lambert, T., Pierson-Wickmann, A. C., Gruau, G., Jaffrezic, A., Petitjean, P., Thibault, J. N., and Jeanneau, L.: Hydrologically driven seasonal changes in the sources and production mechanisms of dissolved organic carbon in a small lowland catchment, Water Resour Res, 49, 5792-5803, 10.1002/wrcr.20466, 2013.

Laudon, H., Buttle, J., Carey, S. K., McDonnell, J., McGuire, K., Seibert, J., Shanley, J., Soulsby, C., and Tetzlaff, D.: Cross-regional prediction of long-term trajectory of stream water DOC response to climate change, Geophys Res Lett, 39, 10.1029/2012gl053033, 2012.

Lawrence, C. R., Harden, J. W., Xu, X. M., Schulz, M. S., and Trumbore, S. E.: Long-term controls on soil organic carbon with depth and time: A case study from the Cowlitz River Chronosequence, WA USA, Geoderma, 247, 73-87, 10.1016/j.geoderma.2015.02.005, 2015.

Lehmann, J., Kinyangi, J., and Solomon, D.: Organic matter stabilization in soil microaggregates: implications from spatial heterogeneity of organic carbon contents and carbon forms, Biogeochemistry, 85, 45-57, 10.1007/s10533-007-9105-3, 2007.

Li, L., Salehikhoo, F., Brantley, S. L., and Heidari, P.: Spatial zonation limits magnesite dissolution in porous media, Geochim Cosmochim Ac, 126, 555-573, 10.1016/j.gca.2013.10.051, 2014.

Li, L., Bao, C., Sullivan, P. L., Brantley, S., Shi, Y., and Duffy, C.: Understanding watershed hydrogeochemistry: 2. Synchronized hydrological and geochemical processes drive stream chemostatic behavior, Water Resour Res, 2017.

Li, L., DiBiase, R. A., Del Vecchio, J., Marcon, V., Hoagland, B., Xiao, D., Wayman, C., Tang, Q., He, Y., Silverhart, P., Forsythe, B., Williams, J. Z., Shapich, D., Mount, G. J., Kaye, J., Guo, L., Lin, H., Eissenstat, D., Dere, A., Brubaker, K., Kaye, M., Davis, K., Russo, T., and Brantley, S.: Investigating the effect of lithology and agriculture at the Susquehanna Shale Hills Critical Zone Observatory (SSHCZO): The Garner Run and Cole Farm subcatchments, Vadose Zone Journal, doi:10.2136/vzj2018.03.0063, 2018.

Li, L.: Watershed reactive transport, in: Reviews in Mineralogy & Geochemistry: REACTIVE TRANSPORT IN NATURAL AND ENGINEERED SYSTEMS, edited by: Druhan, J., and Tournassat, C., Mineralogical Society of America, 2019.

Li, M. X., Peng, C. H., Zhou, X. L., Yang, Y. Z., Guo, Y. R., Shi, G. H., and Zhu, Q. A.: Modeling Global Riverine DOC Flux Dynamics From 1951 to 2015, Journal of Advances in Modeling Earth Systems, 11, 514-530, 10.1002/2018ms001363, 2019.

Lim, K. J., Engel, B. A., Tang, Z. X., Choi, J., Kim, K. S., Muthukrishnan, S., and Tripathy, D.: Automated Web Gis based hydrograph analysis tool, what, Journal of the American Water Resources Association, 41, 1407-1416, 10.1111/j.1752-1688.2005.tb03808.x, 2005.

Lin, H.: Temporal stability of soil moisture spatial pattern and subsurface preferential flow pathways in the shale hills catchment, Vadose Zone J, 5, 317-340, 10.2136/vzj2005.0058, 2006.

Lin, H., and Zhou, X.: Evidence of subsurface preferential flow using soil hydrologic monitoring in the Shale Hills catchment, European Journal of Soil Science, 59, 34-49, 10.1111/j.1365-2389.2007.00988.x, 2008.

Liu, Y., Wang, C. H., He, N. P., Wen, X. F., Gao, Y., Li, S. G., Niu, S. L., Butterbach-Bahl, K., Luo, Y. Q., and Yu, G. R.: A global synthesis of the rate and temperature sensitivity of soil nitrogen mineralization: latitudinal patterns and mechanisms, Glob. Change Biol., 23, 455-464, 10.1111/gcb.13372, 2017.

Malone, E. T., Abbott, B. W., Klaar, M. J., Kidd, C., Sebilo, M., Milner, A. M., and Pinay, G.: Decline in Ecosystem delta C-13 and Mid-Successional Nitrogen Loss in a Two-Century Postglacial Chronosequence, Ecosystems, 21, 1659-1675, 10.1007/s10021-018-0245-1, 2018.

Meybeck, M., and Moatar, F.: Daily variability of river concentrations and fluxes: indicators based on the segmentation of the rating curve, Hydrological Processes, 26, 1188-1207, 10.1002/hyp.8211, 2012.

Michalzik, B., Kalbitz, K., Park, J. H., Solinger, S., and Matzner, E.: Fluxes and concentrations of dissolved organic carbon and nitrogen - a synthesis for temperate forests, Biogeochemistry, 52, 173-205, 10.1023/a:1006441620810, 2001.

Moatar, F., Abbott, B. W., Minaudo, C., Curie, F., and Pinay, G.: Elemental properties, hydrology, and biology interact to shape concentration-discharge curves for carbon, nutrients, sediment, and major ions, Water Resour Res, 53, 1270-1287, 10.1002/2016wr019635, 2017.

Monteith, D. T., Stoddard, J. L., Evans, C. D., de Wit, H. A., Forsius, M., Hogasen, T., Wilander, A., Skjelkvale, B. L., Jeffries, D. S., Vuorenmaa, J., Keller, B., Kopacek, J., and Vesely, J.: Dissolved organic carbon trends resulting from changes in atmospheric deposition chemistry, Nature, 450, 537-U539, 10.1038/nature06316, 2007.

Monteith, D. T., Henrys, P. A., Evans, C. D., Malcolm, I., Shilland, E. M., and Pereira, M. G.: Spatial controls on dissolved organic carbon in upland waters inferred from a simple statistical model, Biogeochemistry, 123, 363-377, 10.1007/s10533-015-0071-x, 2015.

Moriasi, D. N., Arnold, J. G., Van Liew, M. W., Bingner, R. L., Harmel, R. D., and Veith, T. L.: Model evaluation guidelines for systematic quantification of accuracy in watershed simulations, Transactions of the Asabe, 50, 885-900, 2007.

Moyano, F. E., Vasilyeva, N., Bouckaert, L., Cook, F., Craine, J., Yuste, J. C., Don, A., Epron, D., Formanek, P., Franzluebbers, A., Ilstedt, U., Katterer, T., Orchard, V., Reichstein, M., Rey, A., Ruamps, L., Subke, J. A., Thomsen, I. K., and Chenu, C.: The moisture response of soil heterotrophic respiration: interaction with soil properties, Biogeosciences, 9, 1173-1182, 10.5194/bg-9-1173-2012, 2012.

Musolff, A., Schmidt, C., Selle, B., and Fleckenstein, J. H.: Catchment controls on solute export, Adv Water Resour, 86, 133-146, 10.1016/j.advwatres.2015.09.026, 2015.

Musolff, A., Fleckenstein, J. H., Rao, P. S. C., and Jawitz, J. W.: Emergent archetype patterns of coupled hydrologic and biogeochemical responses in catchments, Geophys Res Lett, 44, 4143-4151, 10.1002/2017gl072630, 2017.

Musolff, A., Fleckenstein, J. H., Opitz, M., Büttner, O., Kumar, R., and Tittel, J.: Spatio-temporal controls of dissolved organic carbon stream water concentrations, Journal of Hydrology, 566, 205-215, 10.1016/j.jhydrol.2018.09.011, 2018.

Nash, J. E., and Sutcliffe, J. V.: River flow forecasting through conceptual models part I—A discussion of principles, J Hydrol, 10, 282-290, 1970.

Neff, J. C., and Asner, G. P.: Dissolved organic carbon in terrestrial ecosystems: Synthesis and a model, Ecosystems, 4, 29-48, 10.1007/s100210000058, 2001.

Pacific, V. J., Jencso, K. G., and McGlynn, B. L.: Variable flushing mechanisms and landscape structure control stream DOC export during snowmelt in a set of nested catchments, Biogeochemistry, 99, 193-211, 10.1007/s10533-009-9401-1, 2010.

Perdrial, J., Brooks, P. D., Swetnam, T., Lohse, K. A., Rasmussen, C., Litvak, M., Harpold, A. A., Zapata-Rios, X., Broxton, P., Mitra, B., Meixner, T., Condon, K., Huckle, D., Stielstra, C., Vázquez-Ortega, A., Lybrand, R., Holleran, M., Orem, C., Pelletier, J., and Chorover, J.: A net ecosystem carbon budget for snow dominated forested headwater catchments: linking water and carbon fluxes to critical zone carbon storage, Biogeochemistry, 138, 225-243, 10.1007/s10533-018-0440-3, 2018.

Perdrial, J. N., McIntosh, J., Harpold, A., Brooks, P. D., Zapata-Rios, X., Ray, J., Meixner, T., Kanduc, T., Litvak, M., Troch, P. A., and Chorover, J.: Stream water carbon controls in seasonally snow-covered mountain catchments: impact of inter-annual variability of water fluxes, catchment aspect and seasonal processes, Biogeochemistry, 118, 273-290, 10.1007/s10533-013-9929-y, 2014.

Piney, G., Bernal, S., Abbott, B. W., Lupon, A., Marti, E., Sabater, F., and Krause, S.: Riparian Corridors: A New Conceptual Framework for Assessing Nitrogen Buffering Across Biomes, Frontiers in Environmental Science, 6, 10.3389/fenvs.2018.00047, 2018.

Radke, A. G., Godsey, S. E., Lohse, K. A., McCorkle, E. P., Perdrial, J., Seyfried, M. S., and Holbrook, W. S.: Spatiotemporal Heterogeneity of Water Flowpaths Controls Dissolved Organic Carbon Sourcing in a Snow-Dominated, Headwater Catchment, Frontiers in Ecology and Evolution, 7, 10.3389/fevo.2019.00046, 2019.

Rasmussen, C., Heckman, K., Wieder, W. R., Keiluweit, M., Lawrence, C. R., Berhe, A. A., Blankinship, J. C., Crow, S. E., Druhan, J. L., Hicks Pries, C. E., Marin-Spiotta, E., Plante, A. F., Schädel, C., Schimel, J. P., Sierra,

C. A., Thompson, A., and Wagai, R.: Beyond clay: towards an improved set of variables for predicting soil organic matter content, Biogeochemistry, 137, 297-306, 10.1007/s10533-018-0424-3, 2018.
Raymond, P. A., Saiers, J. E., and Sobczak, W. V.: Hydrological and biogeochemical controls on watershed dissolved organic matter transport: pulse-shunt concept, Ecology, 97, 5-16, 10.1890/14-1684.1, 2016.
Regnier, P., Friedlingstein, P., Ciais, P., Mackenzie, F. T., Gruber, N., Janssens, I. A., Laruelle, G. G., Lauerwald, R., Luyssaert, S., Andersson, A. J., Arndt, S., Arnosti, C., Borges, A. V., Dale, A. W., Gallego-Sala, A., Godderis, Y., Goossens, N., Hartmann, J., Heinze, C., Ilyina, T., Joos, F., LaRowe, D. E., Leifeld, J., Meysman, F. J. R., Munhoven, G., Raymond, P. A., Spahni, R., Suntharalingam, P., and Thullner, M.: Anthropogenic perturbation of the carbon fluxes from land to ocean, Nature Geoscience, 6, 597-607, 10.1038/ngeo1830, 2013.
Sadiq, R., and Rodriguez, M. J.: Disinfection by-products (DBPs) in drinking water and predictive models for their occurrence: a review, Science of The Total Environment, 321, 21-46, 10.1016/j.scitotenv.2003.05.001, 2004.
Seibert, J., Grabs, T., Köhler, S., Laudon, H., Winterdahl, M., and Bishop, K.: Linking soil- and stream-water chemistry based on a Riparian Flow-Concentration Integration Model, Hydrology and earth system sciences, 13, 2287-2297, 2009.
Shi, Y. N., Davis, K. J., Duffy, C. J., and Yu, X.: Development of a Coupled Land Surface Hydrologic Model and Evaluation at a Critical Zone Observatory, Journal of Hydrometeorology, 14, 1401-1420, 10.1175/jhm-d-12-0145.1, 2013.
Skjelkvale, B. L., Stoddard, J. L., Jeffries, D. S., Torseth, K., Hogasen, T., Bowman, J., Mannio, J., Monteith, D. T., Mosello, R., Rogora, M., Rzychon, D., Vesely, J., Wieting, J., Wilander, A., and Worsztynowicz, A.: Regional scale evidence for improvements in surface water chemistry 1990-2001, Environ. Pollut., 137, 165-176, 10.1016/j.envpol.2004.12.023, 2005.
Smith, K. A., Ball, T., Conen, F., Dobbie, K. E., Massheder, J., and Rey, A.: Exchange of greenhouse gases between soil and atmosphere: interactions of soil physical factors and biological processes, European Journal of Soil Science, 54, 779, 10.1046/j.1351-0754.2003.0567.x, 2003.
Stielstra, C., Brooks, P. D., Lohse, K. A., McIntosh, J. M., Chorover, J., Barron-Gafford, G., Perdrial, J. N., Barnard, H. R., and Litvak, M.: Climatic and landscape influences on soil moisture are primary determinants of soil carbon fluxes in seasonally snow-covered forest ecosystems, Biogeochemistry, 123, 447-465, 10.1007/s10533-015-0078-3, 2015.
Stockmann, U., Adams, M. A., Crawford, J. W., Field, D. J., Henakaarchchi, N., Jenkins, M., Minasny, B., McBratney, A. B., de Courcelles, V. D., Singh, K., Wheeler, I., Abbott, L., Angers, D. A., Baldock, J., Bird, M., Brookes, P. C., Chenu, C., Jastrow, J. D., Lal, R., Lehmann, J., O'Donnell, A. G., Parton, W. J., Whitehead, D., and Zimmermann, M.: The knowns, known unknowns and unknowns of sequestration of soil organic carbon, Agriculture Ecosystems & Environment, 164, 80-99, 10.1016/j.agee.2012.10.001, 2013.
Temnerud, J., von Bromssen, C., Folster, J., Buffam, I., Andersson, J. O., Nyberg, L., and Bishop, K.: Map-based prediction of organic carbon in headwater streams improved by downstream observations from the river outlet, Biogeosciences, 13, 399-413, 10.5194/bg-13-399-2016, 2016.
Thomas, Z., Abbott, B., Troccaz, O., Baudry, J., and Pinay, G.: Proximate and ultimate controls on carbon and nutrient dynamics of small agricultural catchments, Biogeosciences, 13, 1863-1875, 10.5194/bg-13-1863-2016, 2016.
Underwood, K. L., Rizzo, D. M., Schroth, A. W., and Dewoolkar, M. M.: Evaluating Spatial Variability in Sediment and Phosphorus Concentration-Discharge Relationships Using Bayesian Inference and Self-Organizing Maps, Water Resour Res, 53, 10293-10316, 10.1002/2017wr021353, 2017.
Weigand, S., Bol, R., Reichert, B., Graf, A., Wiekenkamp, I., Stockinger, M., Luecke, A., Tappe, W., Bogena, H., Puetz, T., Amelung, W., and Vereecken, H.: Spatiotemporal Analysis of Dissolved Organic Carbon and

https://doi.org/10.5194/hess-2019-310
Preprint. Discussion started: 18 July 2019

Nitrate in Waters of a Forested Catchment Using Wavelet Analysis, Vadose Zone J, 16, 10.2136/vzj2016.09.0077, 2017.
Weiler, M., and McDonnell, J. J.: Testing nutrient flushing hypotheses at the hillslope scale: A virtual experiment approach, Journal of Hydrology, 319, 339-356, 10.1016/j.jhydrol.2005.06.040, 2006.
Western, A. W., Bloschl, G., and Grayson, R. B.: Toward capturing hydrologically significant connectivity in spatial patterns, Water Resour Res, 37, 83-97, 10.1029/2000wr900241, 2001.
Winterdahl, M., Erlandsson, M., Futter, M. N., Weyhenmeyer, G. A., and Bishop, K.: Intra-annual variability of organic carbon concentrations in running waters: Drivers along a climatic gradient, Global Biogeochemical Cycles, 28, 451-464, 10.1002/2013GB004770, 2014.
Winterdahl, M., Laudon, H., Lyon, S. W., Pers, C., and Bishop, K.: Sensitivity of stream dissolved organic carbon to temperature and discharge: Implications of future climates, Journal of Geophysical Research: Biogeosciences, 121, 126-144, 10.1002/2015JG002922, 2016.
Worrall, F., Howden, N. J. K., Burt, T. P., and Bartlett, R.: Declines in the dissolved organic carbon (DOC) concentration and flux from the UK, J Hydrol, 556, 775-789, 10.1016/j.jhydrol.2017.12.001, 2018.
Xiao, D., Shi, Y., Brantley, S., Forsythe, B., DiBiase, R., Davis, K., and Li, L.: Predominant control of soil properties in storage-discharge relationship in catchments derived from contrasting lithologies, Water Resour Res, Under Review, 2019.
Yan, Z. F., Liu, C. X., Todd-Brown, K. E., Liu, Y. Y., Bond-Lamberty, B., and Bailey, V. L.: Pore-scale investigation on the response of heterotrophic respiration to moisture conditions in heterogeneous soils, Biogeochemistry, 131, 121-134, 10.1007/s10533-016-0270-0, 2016.
Yan, Z. F., Bond-Lamberty, B., Todd-Brown, K. E., Bailey, V. L., Li, S. L., Liu, C. Q., and Liu, C. X.: A moisture function of soil heterotrophic respiration that incorporates microscale processes, Nature Communications, 9, 10.1038/s41467-018-04971-6, 2018.
Zarnetske, J. P., Bouda, M., Abbott, B. W., Saiers, J., and Raymond, P. A.: Generality of Hydrologic Transport Limitation of Watershed Organic Carbon Flux Across Ecoregions of the United States, Geophys Res Lett, 45, 11702-11711, 10.1029/2018gl080005, 2018.
Zhi, W., Li, L., Dong, W., Brown, W., Kaye, J., Steefel, C., and Williams, K. H.: Distinct Source Water Chemistry Shapes Contrasting Concentration-Discharge Patterns, Water Resour Res, 55, 4233-4251, 10.1029/2018WR024257, 2019.